TRAINING ON TEST PROTEINS IMPROVES FITNESS, STRUCTURE, AND FUNCTION PREDICTION

Anton Bushuiev[1*]   **Roman Bushuiev**[1,2*]   **Nikola Zadorozhny**[1]   **Raman Samusevich**[1,2]
Hannes Stärk[3]   **Jiri Sedlar**[1]   **Tomáš Pluskal**[2]   **Josef Sivic**[1]

[1]Czech Institute of Informatics, Robotics and Cybernetics, Czech Technical University
[2]Institute of Organic Chemistry and Biochemistry of the Czech Academy of Sciences
[3]CSAIL, Massachusetts Institute of Technology

ABSTRACT

Data scarcity and distribution shifts often hinder the ability of machine learning models to generalize when applied to proteins and other biological data. Self-supervised pre-training on large datasets is a common method to enhance generalization. However, striving to perform well on all possible proteins can limit model's capacity to excel on any specific one, even though practitioners are often most interested in accurate predictions for the individual protein they study. To address this limitation, we propose an orthogonal approach to achieve generalization. Building on the prevalence of self-supervised pre-training, we introduce a method for self-supervised fine-tuning at test time, allowing models to adapt to the test protein of interest on the fly and without requiring any additional data. We study our test-time training (TTT) method through the lens of perplexity minimization and show that it consistently enhances generalization across different models, their scales, and datasets. Notably, our method leads to new state-of-the-art results on the standard benchmark for protein fitness prediction, improves protein structure prediction for challenging targets, and enhances function prediction accuracy.

1 INTRODUCTION

A comprehensive understanding of protein structure, function, and fitness is essential for advancing research in the life sciences (Subramaniam & Kleywegt, 2022; Tyers & Mann, 2003; Papkou et al., 2023). While machine learning models have demonstrated remarkable potential in protein research, they are typically optimized for achieving the best average performance across large datasets (Jumper et al., 2021; Watson et al., 2023; Yang et al., 2024; Kouba et al., 2023). However, biologists often focus their research on individual proteins or protein complexes involved for example in metabolic disorders (Ashcroft et al., 2023; Gunn & Neher, 2023), oncogenic signalling (Hoxhaj & Manning, 2020; Keckesova et al., 2017), neurodegeneration (Gulen et al., 2023; oh Seo et al., 2023), and other biological phenomena (Gu et al., 2022). In these scenarios, detailed insights into a single protein can lead to significant scientific advances.

Nonetheless, general machine learning models for proteins often struggle to generalize to individual case studies due to data

ESMFold   **ESMFold + TTT**

Perplexity: **13.0**   Perplexity: **3.0**
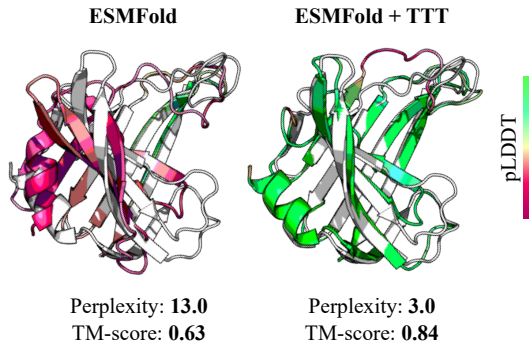TM-score: **0.63**   TM-score: **0.84**

Figure 1: **Example of test-time training (TTT) applied to protein folding.** ESMFold poorly predicts the structure of the CASP14 target T1074 (shown in white) because the underlying language model ESM2 poorly fits the sequence, as indicated by the high perplexity (Fig. 2E in Lin et al. (2023) and the left panel here). Self-supervised test-time training of ESM2 on the single sequence of T1074 directly minimizes the perplexity, leading to improved structure prediction (better TM-score alignment and higher pLDDT predicted confidence). The same test-time training approach is also broadly applicable to other tasks, such as protein fitness and function prediction.

---

scarcity (Bushuiev et al., 2023; Chen & Gong, 2022) and distribution shifts (Tagasovska et al., 2024; Feng et al., 2024). Bridging the gap between broad, dataset-wide optimizations and the precision required for studying single proteins in practical applications remains a critical challenge in integrating machine learning into biological research (Sapoval et al., 2022).

By contrast, in other application domains of machine learning, such as computer vision and natural language processing, customization and adaptation approaches have emerged as powerful tools to improve model performance in specific contexts (Ruiz et al., 2023; Hardt & Sun, 2023). Drawing inspiration from the test-time training (TTT) approach developed in computer vision to mitigate distribution shifts (Sun et al., 2020; Gandelsman et al., 2022), in this work we propose the TTT approach for proteins. Our method enables adapting protein models to one protein at a time, on the fly, and without the need for additional data. Given a model that has been pre-trained using masked language modeling, our method minimizes the perplexity of the model on a given test protein through self-supervised fine-tuning, which, in turn, results in improved downstream performance without updating the downstream task head.

The prevalence of masked modeling in protein machine learning makes our method broadly applicable to various downstream tasks. Empirically, we demonstrate its effectiveness across three key challenges in protein machine learning. First, TTT achieves state-of-the-art results on the ProteinGym dataset (Notin et al., 2024), a well-established benchmark for protein fitness prediction. Second, TTT enhances protein structure predictions with ESMFold (Lin et al., 2023) and ESM3 (Hayes et al., 2024) on challenging targets. Third, the application of TTT to protein function predictors results in improved classification of terpene synthase (TPS) substrates and protein subcellular localization.

In summary, the key contributions of this work are three-fold:

1. Motivated by the generalization challenges and distribution shifts prevalent in protein machine learning, we introduce a new test-time training (TTT) method[1] that enables models to adapt to individual proteins on the fly and without requiring additional data.

2. We establish a link between our TTT approach and perplexity minimization, providing an insight into why this approach enhances model effectiveness.

3. We empirically validate TTT, achieving state-of-the-art results in protein fitness prediction, improving the protein structure prediction capabilities of well-established folding models, and enhancing protein function predictions in the tasks of terpene synthase substrate classification and protein localization prediction.

2 BACKGROUND AND RELATED WORK

In this section, we present the context and related work that highlight the feasibility and broad applicability of test-time training (TTT) in the domain of machine learning on proteins. The widespread adoption of Y-shaped architectures relying on masked modeling enables the development of a general method for adapting protein models at test time via masking-based self-supervised fine-tuning.

The Y-shaped paradigm of learning. In machine learning applied to biology, architectures often follow a Y-shaped paradigm (Gandelsman et al., 2022), consisting of a backbone feature extractor f, a self-supervised head g, and an alternative fine-tuning head h. During training, $g \circ f$ is first pre-trained, after which the pre-trained backbone f is reused to fine-tune $h \circ f$ toward a downstream task. Here, $\circ$ denotes a composition of two machine learning modules (e.g., g is applied on top of f in $g \circ f$). At test time, the final model $h \circ f$ is fixed. Generalization is achieved by leveraging the rich knowledge encoded in the backbone f and the task-specific priors acquired in the fine-tuning head h. This paradigm enables overcoming data scarcity during fine-tuning and underlies breakthrough approaches in protein structure prediction (Lin et al., 2023), protein design (Watson et al., 2023), protein function prediction (Yu et al., 2023), and other protein-related tasks (Hayes et al., 2024).

The backbone f is typically a large neural network pre-trained in a self-supervised way on a large dataset using a smaller pre-training projection head g (Hayes et al., 2024). The fine-tuning head h, however, depends on the application. In some cases, h is a large neural network, repurposing the

---

[1]https://github.com/anton-bushuiev/ProteinTTT

pre-trained model entirely (Watson et al., 2023; Lin et al., 2023); in others, h is a minimal projection with few parameters (Cheng et al., 2023), or even without any parameters at all (i.e., a zero-shot setup, (Meier et al., 2021; Dutton et al., 2024)). In some cases, the fine-tuning head h may also be a machine learning algorithm other than a neural network (Samusevich et al., 2024).

Masked modeling.   While the objective of fine-tuning $h \circ f$ is determined by the downstream application, the choice of pre-training objective for $g \circ f$ is less straightforward. Nevertheless, most methods employ various forms of masked modeling, i.e., optimizing the model weights to accurately reconstruct missing parts of proteins, regardless of the downstream application. Masked modeling pre-traning underpins models for protein structure (Lin et al., 2023) and function (Samusevich et al., 2024) prediction, as well as for protein design (Hayes et al., 2024). For example, in AlphaFold2, most of the loss function weight is put onto masked modeling of multiple sequence alignments (MSAs) (Jumper et al., 2021), and the model has been effectively fine-tuned for various tasks beyond structure prediction (Jing et al., 2024; Cheng et al., 2023; Motmaen et al., 2023).

Masked modeling is a dominant pre-training objective not only across different tasks but also across various protein representations. Sequence models applied to proteins are typically pre-trained to predict randomly masked amino acids in a random or autoregressive manner (Lin et al., 2023; Rao et al., 2021; Elnaggar et al., 2023; Madani et al., 2023; Ferruz et al., 2022; Rives et al., 2021; Rao et al., 2020). Models utilizing graph neural networks or 3D convolutions on protein structures are also commonly pre-trained to fill in missing structural fragments (Dieckhaus et al., 2024; Diaz et al., 2023; Bushuiev et al., 2023; Hsu et al., 2022; Shroff et al., 2020). The most recent approaches combine both sequential and structural information under masked modeling (Hayes et al., 2024; Su et al., 2023; Heinzinger et al., 2023).

Model adaptation.   In many scenarios, machine learning models for proteins benefit from being adapted to a specific protein of interest. This adaptation is commonly achieved in two ways: either via additional input features or via protein-specific fine-tuning. Multiple sequence alignments (MSAs) containing sequences similar to the target protein provide a common way of supplying a model with protein-specific features (Abramson et al., 2024; Jumper et al., 2021; Rao et al., 2021). Another approach for injecting protein-specific knowledge into the model is standard supervised fine-tuning (i.e., via the $h \circ f$ track) on protein-specific data (Notin et al., 2024; Kirjner et al., 2023; Rao et al., 2019). An alternative is self-supervised fine-tuning (i.e., via the $g \circ f$ track) on proteins from the MSA (Notin et al., 2022b; Frazer et al., 2021; Alley et al., 2019) or on proteins sharing another property with the target protein, such as common family (Sevgen et al., 2023) or class (Samusevich et al., 2024). However, constructing MSAs is time-consuming (Fang et al., 2023), and similar proteins may not be available for many targets (Durairaj et al., 2023; Lin et al., 2023).

Here, we propose an extreme case of self-supervised fine-tuning: learning from a single target protein, without the need for any additional data. To the best of our knowledge, this approach has not been employed in the field of machine learning applied to biology; however, similar methods have been developed in computer vision (Chi et al., 2024; Wang et al., 2023; Xiao et al., 2022; Karani et al., 2021) and natural language processing (Hardt & Sun, 2023; Ben-David et al., 2022; Banerjee et al., 2021). The paradigm of test-time training (TTT), developed to mitigate distribution shifts in computer vision applications (Gandelsman et al., 2022; Sun et al., 2020), is a main inspiration for our work. Here, we demonstrate that TTT is highly relevant for machine learning on proteins even without the presence of explicit distribution shift. We investigate the link of TTT to perplexity minimization and show that TTT improves performance on several downstream tasks.

3   TEST-TIME TRAINING (TTT) ON PROTEINS

As discussed in the previous section, many machine learning models for proteins employ Y-shaped architectures, consisting of a backbone f with a self-supervised head g and a supervised head h. This design facilitates the use of self-supervised fine-tuning across various tasks and models. Notably, most of these models leverage masked modeling as a pre-training objective, which enables the introduction of a broadly applicable test-time training (TTT) method based on masking. Our method adapts models to specific test proteins through masked modeling (Figure 2). In this section, we first formally define the proposed TTT approach (Section 3.1), followed by its application to a range of
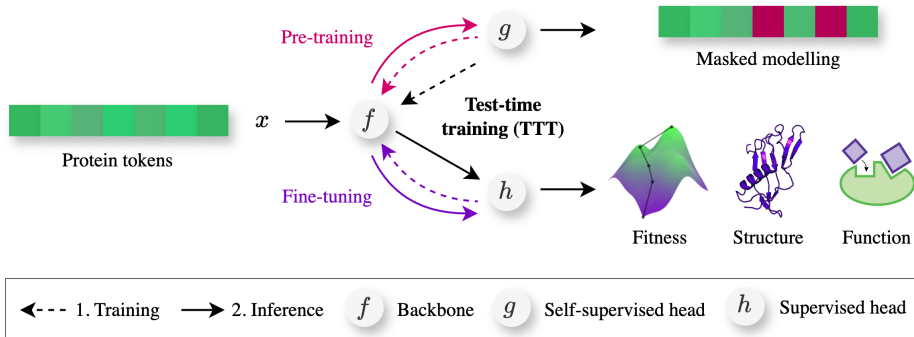
Figure 2: **Overview of our test-time training (TTT) for proteins.** Test-time training for proteins builds on the prevalence of Y-shaped architectures relying on masked modeling (i.e., self-supervised masking-based pre-training of $g \circ f$ followed by supervised fine-tuning of $h \circ f$, sharing the backbone f). Given a single test protein x, TTT adapts the backbone f to the protein using self-supervised fine-tuning. This adaptation leads to better generalization for the downstream task, such as protein fitness, structure, or function prediction.

well-established models (Section 3.2). Finally, we provide an insight into the effectiveness of our method by linking it to perplexity minimization (Section 3.3).

3.1 SELF-SUPERVISED FINE-TUNING ON TEST PROTEINS

At test time, we assume a Y-shaped model with a backbone f that has been pre-trained via the self-supervised track $g \circ f$, followed by task-specific fine-tuning through the supervised track $h \circ f$. The goal of test-time training (TTT) is to adapt the backbone f to a single test example x before performing test-time inference on a downstream task via the supervised track.

To achieve this, we first fine-tune the backbone f using the self-supervised track $g \circ f$ on the single example x. This step customizes the backbone f to the test sample x, and, as demonstrated in Section 4, enhances the generalization of $h \circ f$ without modifying the weights of the task-specific head h. Figure 2 illustrates our method. Although the concept of TTT is relatively simple, it involves several important design choices, such as selecting the optimizer and efficiently fine-tuning large backbones, which we describe in the following paragraphs.

Training objective. We fine-tune $g \circ f$ on a test sample x via minimizing the masked language modeling objective (Devlin, 2018; Rives et al., 2021):

$$\mathcal{L}(x) = \mathbb{E}_M \left[\sum_{i \in M} - \log p(x_i | x_{\setminus M}) \right], \tag{1}$$

where x denotes a sequence of protein tokens (typically amino acid types), and $\mathbb{E}_M$ represents the expectation over randomly sampled masking positions M. The loss function $\mathcal{L}(x)$ maximizes the log-probabilities $\log p(x_i | x_{\setminus M})$ of the true tokens x_i at the masked positions $i \in M$ in the partially masked sequence $x_{\setminus M}$. Please note that here we focus on bi-directional masked modeling models, which employ random masking, but the method can be straightforwardly extended to models employing autoregressive masking.

In practice, $\mathbb{E}_M$ can follow different distributions, such as sampling a fixed proportion (e.g., 15%) of random amino acid tokens (Lin et al., 2023), or dynamically varying the number of sampled tokens based on another distribution (e.g., a beta distribution) (Hayes et al., 2024). During test-time training, we replicate the masking distribution used during the pre-training. If relevant, we also replicate other pre-training tricks, such as replacing 10% of masked tokens with random tokens and another 10% with the original tokens (Devlin, 2018; Lin et al., 2023; Su et al., 2023) or cropping sequences to random 1024-token fragments (Lin et al., 2023; Su et al., 2023).

Optimization. We minimize the loss defined in Equation (1) using stochastic gradient descent (SGD) with zero momentum and zero weight decay (Ruder, 2016). While a more straightforward
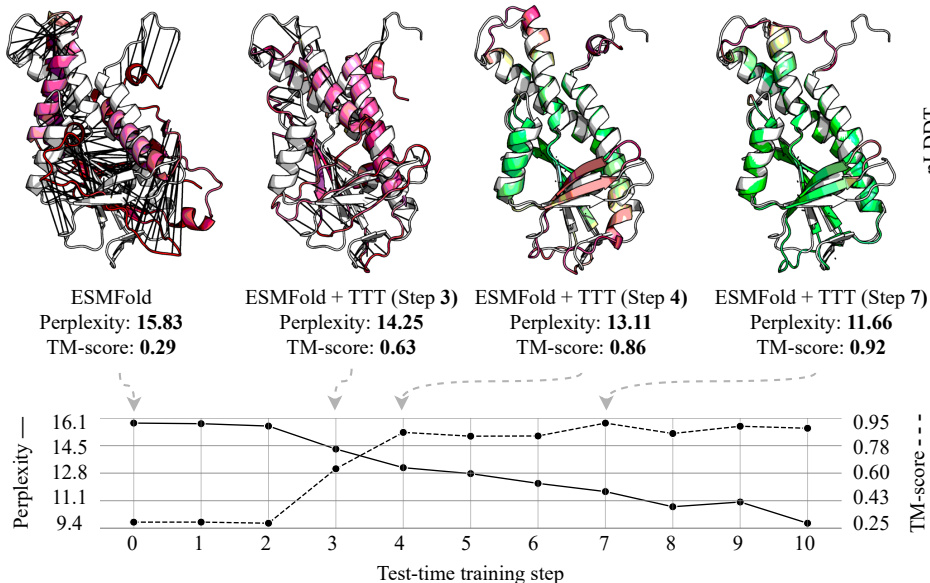
Figure 3: **Test-time training (TTT) improves protein structure prediction by reducing protein sequence perplexity**. ESMFold fails to predict the structure of chain B from PDB entry 7EBL in the CAMEO validation set, as shown at TTT step 0, where the perplexity is high and the TM-score is low. By applying TTT on the single target sequence, the model iteratively improves the structure prediction quality, as demonstrated by the increasing TM-score, associated with reduced perplexity. At step 7, the predicted structure achieves the highest TM-score, as well as the highest predicted confidence metric pLDDT, enabling the selection of this step as the final prediction by ESMFold + TTT.

option might be to use the optimizer state from the final pre-training step, this approach is often impractical because the optimizer parameters are usually not provided with the pre-trained model weights (Hayes et al., 2024; Lin et al., 2023). Moreover, many models are pre-trained using the Adam optimizer (Kingma & Ba, 2015) or its variants (Loshchilov & Hutter, 2019). However, it has been shown that Adam results in less predictable behavior of test-time training (TTT) compared to the SGD optimizer, possibly due to its more exploratory behavior (Gandelsman et al., 2022).

Because each TTT experiment assumes only one test example available, we are not able to halt the training using early stopping on any validation sample. Therefore, for each choice of task-specific f and h, we tune the optimal number of TTT steps using the entire validation set beforehand or rely on available performance estimates (e.g., pLDDT in the case of protein structure prediction; Section 4.2) to select the optimal number of optimization steps.

Fine-tuning large models. We aim for test-time training to be applicable on the fly, i.e., without the need for any pre-computation and on a single GPU with a minimum computational overhead. This poses two challenges when using large models. First, when using pre-trained transformers on a single GPU, even for the forward pass, the batch size is typically limited to only several samples due to the quadratic complexity of the inference (Vaswani, 2017). Second, for the backward pass, even a batch size of one is not always feasible for large models. To address the first challenge, we perform forward and backward passes through a small number of training examples and accumulate gradients to simulate updates with any batch size. We address the second challenge by employing low-rank adaptation (LoRA, Hu et al. (2021)), which in practice enables fine-tuning of any model for which a forward pass on a single sample is feasible, due to a low number of trainable parameters.

3.2 INFERENCE ON DOWNSTREAM TASKS

Once the backbone f is adapted to a test protein via self-supervised fine-tuning, it can be used in conjunction with a pre-trained downstream head h, as $h \circ f$. The key idea of TTT is not to update the head h during test time, but rather to leverage improved input representations from f.

Since Y-shaped architectures are prevalent in protein machine learning, TTT can be straightforwardly applied to numerous tasks in protein research. In this work, we address three primary challenges: protein fitness, structure, and function prediction, applying TTT to corresponding well-established models. For fitness prediction, we apply TTT to ESM2 (Lin et al., 2023) and SaProt (Su et al., 2023); for folding, we apply it to ESMFold (Lin et al., 2023) and ESM3 (Hayes et al., 2024); and for function prediction, we apply TTT to ESM-1v-based (Meier et al., 2021) TerpeneMiner (Samusevich et al., 2024) and ESM-1b-based (Rives et al., 2021) Light attention (Stärk et al., 2021).

In all the models we consider, f is a transformer encoder that takes a protein sequence as input (except for SaProt, which also uses structural tokens), while g is a masked language modeling head (a layer mapping token embeddings to amino acid types). The downstream task heads h, however, vary significantly across tasks. For fitness prediction, h outputs a single value for a mutated sequence, measuring how well the protein supports an organism's functioning. Both ESM2 and SaProt use zero-shot inference from $g \circ f$ via log odds, where h is a simple adaptation of g without any additional parameters. For structure prediction, h is a protein structure decoder: in ESMFold, it is an AlphaFold2-like structure prediction module (Jumper et al., 2021), while in ESM3, it is a VQ-VAE decoder (Razavi et al., 2019). The function predictors are classification models: in TerpeneMiner (Samusevich et al., 2024), h is a random forest that outputs substrate probabilities, and in Light attention (Stärk et al., 2021), h is a light attention module predicting localization class probabilities. Detailed descriptions of the models and their TTT adaptation are provided in Appendix A.

3.3 LINK BETWEEN TEST-TIME TRAINING AND PERPLEXITY MINIMIZATION

While the approach of test-time training has been extensively investigated in computer vision and other domains, the reasons behind its effectiveness remain unclear (Liu et al., 2021; Zhao et al., 2023). Here, we offer a potential explanation by linking test-time training to perplexity minimization within the context of protein sequence modeling.

Perplexity has traditionally been used in natural language processing to evaluate how well models comprehend test sentences (Brown, 2020; Chelba et al., 2013). Protein language modeling has adopted this metric to assess how effectively models understand amino acid sequences (Hayes et al., 2024; Lin et al., 2023). For bidirectional, random masking language models, which are the focus of this study, we consider the following definition of perplexity [2]:
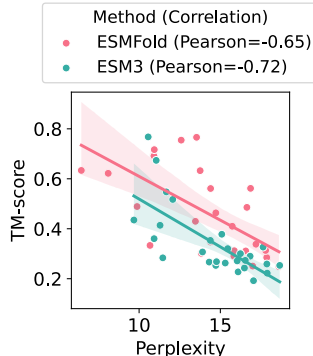

Figure 4: The quality of protein structure prediction, as measured by TM-score, correlates with the perplexity of the underlying language model on the challenging targets from the CAMEO validation set. Higher TM-scores are associated with lower perplexity, indicating that better predictions are linked to lower uncertainty in the language model's understanding of the protein sequence.

$$\text{Perplexity}(x) = \exp\left(\frac{1}{|x|}\sum_{i=1}^{|x|} -\log p(x_i|x_{\setminus i})\right), \quad (2)$$

where $|x|$ is the length of the input protein sequence x and $p(x_i|x_{\setminus i})$ represents the probability that the model correctly predicts the token x_i at position i when it is masked on the input $x_{\setminus i}$. Perplexity ranges from 1 to infinity (the lower the better), providing an intuitive measure of how well a model understands, on average, positions within a given sequence. A perplexity value of 1 indicates that the model perfectly understands the sequence, accurately predicting all the true tokens.

Several studies have shown that lower perplexity on held-out protein sequences (calculated through the self-supervised track $g \circ f$) correlates with better performance on downstream tasks (via the supervised track $h \circ f$), such as predicting protein contacts (Rao et al., 2020), structure (Lin et al., 2023), or fitness (Kantroo et al., 2024). To provide an example, we analyze the correlation between perplexity and structure prediction performance (Figure 4). A strong correlation suggests that

---

[2]Please note that this is an approximation of perplexity, which is computationally intractable for bidirectional models, and is often referred to as pseudo-perplexity (Lin et al., 2023; Salazar et al., 2019).

reducing a model's perplexity on a single test sample x can lead to improved performance on the downstream task (Figure 3; Figure 11).

Since we consider only a single test example x, the minimization of the masked language modeling loss $\mathcal{L}(x)$ (Equation (1)) on this example is directly linked to minimizing the perplexity Perplexity(x) (Equation (2)). For instance, in the case of a single masked position (i.e., $|M| = 1$), the loss is equal to the logarithm of perplexity. More generally, it can be shown formally that by minimizing the masked language modeling objective, one learns to approximate the conditional marginals of the language (of proteins), including the leave-one-out probabilities evaluated in perplexity (Hennigen & Kim, 2023). As a result, applying test-time training (TTT) through $g \circ f$ enhances the representation of the test protein in the backbone f, leading to improved downstream performance via the fine-tuning track $h \circ f$.

4 EXPERIMENTS

Building on the broad applicability of our test-time training (TTT) approach, we apply it to three example downstream tasks in protein machine learning: fitness, structure, and function prediction. The experimental setup and results for each task are presented in the following subsections.

4.1 PROTEIN FITNESS PREDICTION

Protein fitness refers to the ability of a protein to efficiently perform its biological function, which is determined by its structure, stability, and interactions with other molecules. Predicting protein fitness allows researchers to understand how mutations affect protein function, aiding in protein engineering (Notin et al., 2024). In this paper, we demonstrate that applying test-time training (TTT) to representative models, such as ESM2 (Lin et al., 2023) and SaProt (Su et al., 2023), enhances their protein fitness prediction capabilities. ESM2 is a protein language model trained on protein sequences, while SaProt is an extension of ESM2 that incorporates 3D information via additional structural tokens encoding structures predicted by AlphaFold2 (Jumper et al., 2021).

Evaluation Setup. We evaluate the models using ProteinGym, the standard benchmark for fitness prediction (Notin et al., 2024), focusing specifically on its zero-shot setup. Since the zero-shot setup only provides a test set without any data split, we aim to validate TTT on independent data. To achieve this, we create a new fitness prediction dataset mined from MaveDB, a public repository containing datasets from Multiplexed Assays of Variant Effect (MAVEs) (Esposito et al., 2019). The quality of the new dataset is validated by confirming that both ESM2 and SaProt generalize well to the new data, achieving comparable performance (Appendix A).

Given a protein and its variants, fitness prediction models output one real value per variant to estimate fitness. ProteinGym uses Spearman correlation between predicted and experimentally measured fitness values as the main evaluation metric for assessing the capabilities of models to score mutations. The correlation is first calculated for each protein and then aggregated per types of measured fitness: activity, binding, expression, organismal fitness, and stability. The final Spearman correlation metric is obtained by averaging across these five categories. We adopt this metric in our benchmarking.

In our evaluation, we also include other top-performing baselines on the ProteinGym benchmark: TraceptEVE (Notin et al., 2022b) and GEMME (Laine et al., 2019). TraceptEVE combines language model Tranception (Notin et al., 2022a) with the protein-specific variational autoencoder, EVE, capturing the evolutionary information via MSAs (Frazer et al., 2021). GEMME is a statistical method deriving fitness predictions from evolutionary trees.

Results. Test-time training (TTT) consistently enhances the protein fitness prediction performance of both ESM2 and SaProt models across varying model scales (35M and 650M parameters) and both datasets, test ProteinGym (Table 1 left) and validation MaveDB (Table 6 in Appendix B.2). Notably, SaProt (650M) + TTT sets a new state-of-the-art on the ProteinGym benchmark, achieving a 40% higher improvement compared to the previous leaderboard update (SaProt (650M) against TranceptEVE L). When examining performance across different phenotype categories, TTT yields improvements specifically in the categories where the baseline performance is weakest: "Organismal Fitness", "Binding", and "Activity" (Table 1 right). This improvement indicates the ability of TTT to

Table 1: **Test-time training (TTT) improves protein fitness prediction.** The right section of the table presents performance averaged across individual proteins and then across different protein phenotypes, as classified in the ProteinGym benchmark (Notin et al., 2024). The middle column shows the final performance, averaged across all five phenotype classes. In total, ProteinGym contains 2.5 million mutations across 217 proteins. Standard deviations are calculated over 5 random seeds and, for brevity, omitted in the right panel, where the maximum standard deviation does not exceed 0.0004. Methods marked with an asterisk ("*") are the other top-5 methods in ProteinGym, and the metrics are reproduced from the leaderboard (`https://proteingym.org/benchmarks`).

	Avg. Spearman ↑	Spearman by phenotype ↑				
		Activity	Binding	Expression	Organismal Fitness	Stability
ESM2 (35M) (Lin et al., 2023)	0.3211	0.3137	0.2907	0.3435	0.2184	0.4392
ESM2 (35M) + TTT (Ours)	**0.3407 ± 0.00014**	**0.3407**	**0.2942**	**0.3550**	**0.2403**	**0.4733**
SaProt (35M) (Su et al., 2023)	0.4062	0.3721	0.3568	0.4390	0.2879	0.5749
SaProt (35M) + TTT (Ours)	**0.4106 ± 0.00004**	**0.3783**	**0.3569**	**0.4430**	**0.2955**	**0.5795**
ESM2 (650M) (Lin et al., 2023)	0.4139	0.4254	0.3366	0.4151	0.3691	**0.5233**
ESM2 (650M) + TTT (Ours)	**0.4153 ± 0.00003**	**0.4323**	**0.3376**	**0.4168**	**0.3702**	0.5195
TranceptEVE S* (Notin et al., 2022b)	0.4519	0.4750	0.3957	0.4426	0.4491	0.4973
GEMME* (Laine et al., 2019)	0.4547	0.4820	0.3827	0.4382	0.4517	0.5187
TranceptEVE M* (Notin et al., 2022b)	0.4548	0.4792	0.3858	0.4525	0.4538	0.5025
TranceptEVE L* (Notin et al., 2022b)	0.4559	0.4866	0.3758	0.4574	0.4597	0.5003
SaProt (650M) (Su et al., 2023)	0.4569	0.4584	0.3785	**0.4884**	0.3670	**0.5919**
SaProt (650M) + TTT (Ours)	**0.4583 ± 0.00001**	**0.4593**	**0.3790**	0.4883	**0.3754**	0.5896

enhance predictions on challenging targets. Additionally, we observe an inverse correlation between the degree of TTT enhancement and the depth of the MSA (i.e., the number of available homologous sequences) available for each test protein, suggesting that TTT primarily improves predictions for proteins with fewer similar sequences available in the training data (Table 5 in Appendix B.1).

4.2 PROTEIN STRUCTURE PREDICTION

Protein structure prediction, also known as protein folding, is the task of predicting 3D coordinates of protein atoms given the amino acid sequence. Protein folding is arguably one of the most successful applications of machine learning in the life sciences (Jumper et al., 2021; Lin et al., 2023; Abramson et al., 2024). However, even state-of-the-art protein folding methods struggle to generalize to entirely novel proteins (Kryshtafovych et al., 2023). In this work, we focus on the ESMFold (Lin et al., 2023) and ESM3 (Hayes et al., 2024) models, demonstrating how their performance on challenging protein structures can be boosted by utilizing test-time training.

Evaluation setup. To evaluate the performance of TTT, we use CAMEO, a standard benchmark for protein folding. We use the validation and test folds from Lin et al. (2023), focusing only on challenging targets by filtering them according to standard measures of prediction confidence based on pLDDT and perplexity (Appendix A.2).

Given a protein sequence, the goal of protein folding is to predict 3D coordinates of the protein atoms. To assess the quality of the predicted protein structures with respect to the ground truth structures, we use two standard metrics: TM-score (Zhang & Skolnick, 2004) and LDDT (Mariani et al., 2013). TM-score measures the quality of the global 3D alignment of the target and predicted protein structures, while LDDT is an alignment-free method based on local distance difference tests.

As baseline methods, we use techniques alternative to TTT for improving the performance of the pre-trained base models. In particular, the ESMFold paper proposes randomly masking 15% of amino acids in a protein sequence, allowing for sampling multiple protein structure predictions from the regression ESMFold model (Lin et al., 2023). For each sequence, we sample a number of predictions equal to the total number of TTT steps and refer to this baseline as ESMFold + MP (Masked Prediction). As a baseline for ESM3, we use chain-of-thought iterative decoding, referred to as ESM3 + CoT, proposed in the ESM3 paper (Hayes et al., 2024).

Table 2: **Test-time training (TTT) improves protein structure prediction.** The metrics are averaged across the 18 challenging targets in the CAMEO test set, and standard deviations correspond to 5 random seeds. CoT and MP stand for the chain of though and masked prediction baselines.

	TM-score ↑	LDDT ↑
ESM3 (Hayes et al., 2024)	0.3480 ± 0.0057	0.3723 ± 0.0055
ESM3 + CoT (Hayes et al., 2024)	0.3677 ± 0.0088	0.3835 ± 0.0024
ESM3 + TTT (Ours)	**0.3954 ± 0.0067**	**0.4214 ± 0.0054**
ESMFold (Lin et al., 2023)	0.4649	0.5194
ESMFold + MP (Lin et al., 2023)	0.4862 ± 0.0043	0.5375 ± 0.0070
ESMFold + TTT (Ours)	**0.5047 ± 0.0132**	**0.5478 ± 0.0058**

Results. Test-time training (TTT) consistently improves the performance of both the ESMFold and ESM3 models, outperforming the masked prediction (ESMFold + MP) and chain-of-thought (ESM3 + CoT) baselines, as shown in Table 2. Of the 18 most challenging CAMEO test proteins, ESMFold and ESM3 significantly improved the prediction of 7 and 6 structures, respectively, while only slightly disrupting the prediction of 2 and 1 structures, respectively (Figure 9 in Appendix B.1). Most notably, TTT enables accurate structure prediction for targets that are poorly predicted with original base models. For instance, Figure 1 presents a strongly improved structure predicted using ESMFold + TTT for the target that was part of the CASP14 competition and shown as an unsuccessful case in the original ESMFold publication (Lin et al. (2023), Fig. 2E). Another example is shown in Figure 3, where TTT refined the structure prediction from a low-quality prediction (TM-score = 0.29) to a nearly perfectly folded protein (TM-score = 0.92).

4.3 PROTEIN FUNCTION PREDICTION

Protein function prediction is essential for understanding biological processes and guiding bioengineering efforts (Yu et al., 2023; Radivojac & et al., 2013). However, predicting protein function is challenging due to its vague definition and the scarcity of labeled datasets (Stärk et al., 2021; Mikhael et al., 2024; Samusevich et al., 2024). Therefore, enhancing generalization through TTT is particularly relevant in this context. While improved structure prediction through TTT can already enhance function prediction (Song et al., 2024), we further demonstrate that TTT can facilitate function prediction directly. Specifically, we focus on two tasks: subcellular localization, which predicts a protein's location within a cell (Stärk et al., 2021), and substrate classification for terpene synthases (TPS)—enzymes responsible for the production of terpenoids, the largest class of natural products, and known for their complex biochemistry (Christianson, 2017; Samusevich et al., 2024). Unlike protein fitness or structure prediction, both tasks involve classification (TPS substrate classification being multi-label), providing a complementary evaluation of TTT. We apply TTT to TerpeneMiner (Samusevich et al., 2024) for TPS detection and Light attention (Stärk et al., 2021) for subcellular localization, demonstrating consistent improvements in both tasks.

Evaluation setup. For the terpene substrate classification, we use the largest available dataset of characterized TPS from Samusevich et al. (2024) and repurpose the original cross-validation schema. In the case of protein localization prediction, we use a standard DeepLoc dataset (Almagro Armenteros et al., 2017) as a validation set and setHard from (Stärk et al., 2021) as a test set.

Given a protein, the goal of function prediction is to correctly classify it into one of the predefined functional annotations. We assess the quality of the TPS substrate prediction using standard multi-label classification metrics used in the TerpeneMiner paper (Samusevich et al., 2024): mean average precision (mAP) and area under the receiver operating characteristic curve (AUROC). In the case of protein localization prediction, we similarly use the classification metrics from the original paper (Stärk et al., 2021): accuracy, multi-class Matthews correlation coefficient (MCC), and F1-score.

Results. TTT improves the performance of the base models on both protein function prediction tasks and across all considered metrics (Table 3). Figure 5 provides a qualitative result, where TTT fine-tuning iteratively refines the prediction of TerpeneMiner toward a correct TPS substrate class.
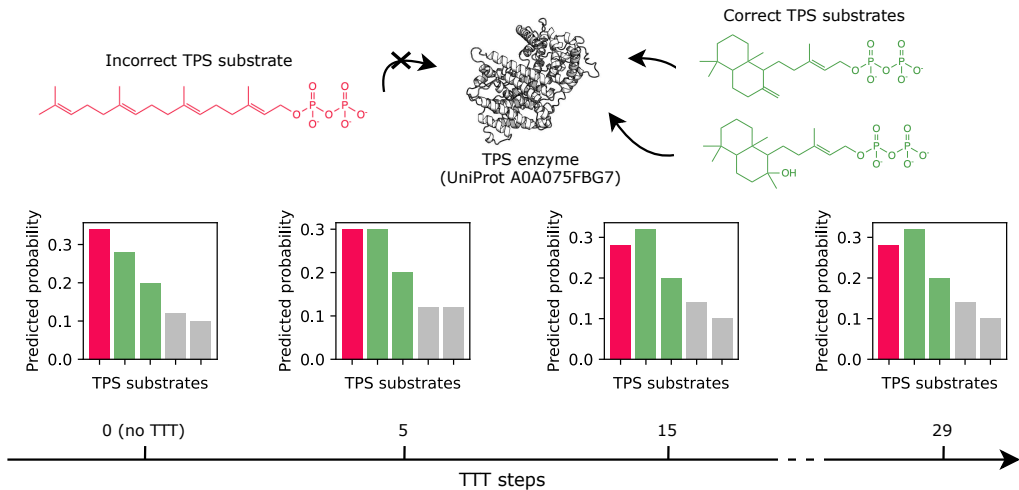
Figure 5: **Test-time training (TTT) enables the correct substrate classification for a terpene synthase (TPS) enzyme.** With progressive test-time training steps of TerpeneMiner + TTT, the probability of the initially misclassified substrate (red) decreases, while the probability of the true substrates (green) increases. The bar plots also display the predicted probabilities for other substrates with non-zero values (grey).

Table 3: **Test-time training (TTT) improves protein function prediction.** For the terpene syntase (TPS) substrate classification task, the metrics are computed on the 512 TPS sequences based on the cross-validation schema of the TPS dataset (Samusevich et al., 2024). Subcellular localization prediction performance is reported for 432 protein sequences from the setHard test set (Stärk et al., 2021). The error bars show standard deviations across five random seeds.

TPS substrate classification		
	mAP ↑	AUROC ↑
TerpeneMiner (Samusevich et al., 2024)	0.805	0.948
TerpeneMiner + TTT (Ours)	**0.811 ± 0.0011**	**0.950 ± 0.0002**

Subcellular localization prediction			
	Accuracy ↑	MCC ↑	F1-score ↑
Light attention (Stärk et al., 2021)	0.627	0.549	0.618
Light attention + TTT (Ours)	**0.634 ± 0.004**	**0.557 ± 0.005**	**0.627 ± 0.004**

5 DISCUSSION

In this work, we have developed test-time training (TTT) for proteins, enabling per-protein adaptation of machine learning models for enhanced generalization. TTT improves performance across models, their scales, and benchmarks, while primarily enhancing performance on challenging targets. Our results open up the field of self-supervised adaptation for proteins and provide a proof-of-concept for other biology-related domains. While our method demonstrated strong potential, several underexplored directions remain for future work. In particular, gaining a comprehensive understanding of the success and failure modes of TTT and its application to emerging foundation models could unlock its full potential in computational biology. Additionally, our findings motivate future investigation of broader adaptation frameworks in the context of proteins. Among these frameworks are, for example, domain adaptation, where models leverage both training and test data to adapt to new domains (Ganin & Lempitsky, 2015), or adaptive risk minimization, which employs meta-learning to derive models that can adapt in the face of domain shifts (Zhang et al., 2021).

REFERENCES

Josh Abramson, Jonas Adler, Jack Dunger, Richard Evans, Tim Green, Alexander Pritzel, Olaf Ronneberger, Lindsay Willmore, Andrew J Ballard, Joshua Bambrick, et al. Accurate structure prediction of biomolecular interactions with alphafold 3. *Nature*, pp. 1–3, 2024.

Ethan C Alley, Grigory Khimulya, Surojit Biswas, Mohammed AlQuraishi, and George M Church. Unified rational protein engineering with sequence-based deep representation learning. *Nature methods*, 16(12):1315–1322, 2019.

José Juan Almagro Armenteros, Casper Kaae Sønderby, Søren Kaae Sønderby, Henrik Nielsen, and Ole Winther. Deeploc: prediction of protein subcellular localization using deep learning. *Bioinformatics*, 33(21):3387–3395, 2017.

Frances M. Ashcroft, Matthew Lloyd, and Elizabeth A. Haythorne. Glucokinase activity in diabetes: too much of a good thing? *Trends in Endocrinology & Metabolism*, 34(2):119–130, Feb 2023. ISSN 1043-2760. doi: 10.1016/j.tem.2022.12.007. URL https://doi.org/10.1016/j.tem.2022.12.007.

Pratyay Banerjee, Tejas Gokhale, and Chitta Baral. Self-supervised test-time learning for reading comprehension. *arXiv preprint arXiv:2103.11263*, 2021.

Eyal Ben-David, Nadav Oved, and Roi Reichart. Pada: Example-based prompt learning for on-the-fly adaptation to unseen domains. *Transactions of the Association for Computational Linguistics*, 10: 414–433, 2022.

Tom B Brown. Language models are few-shot learners. *arXiv preprint arXiv:2005.14165*, 2020.

Anton Bushuiev, Roman Bushuiev, Anatolii Filkin, Petr Kouba, Marketa Gabrielova, Michal Gabriel, Jiri Sedlar, Tomas Pluskal, Jiri Damborsky, Stanislav Mazurenko, et al. Learning to design protein-protein interactions with enhanced generalization. *arXiv preprint arXiv:2310.18515*, 2023.

Ciprian Chelba, Tomas Mikolov, Mike Schuster, Qi Ge, Thorsten Brants, Phillipp Koehn, and Tony Robinson. One billion word benchmark for measuring progress in statistical language modeling. *arXiv preprint arXiv:1312.3005*, 2013.

Tianlong Chen and Chengyue Gong. Hotprotein: A novel framework for protein thermostability prediction and editing. *NeurIPS 2022*, 2022.

Jun Cheng, Guido Novati, Joshua Pan, Clare Bycroft, Akvilė Žemgulytė, Taylor Applebaum, Alexander Pritzel, Lai Hong Wong, Michal Zielinski, Tobias Sargeant, et al. Accurate proteome-wide missense variant effect prediction with alphamissense. *Science*, 381(6664):eadg7492, 2023.

Zhixiang Chi, Li Gu, Tao Zhong, Huan Liu, Yuanhao Yu, Konstantinos N Plataniotis, and Yang Wang. Adapting to distribution shift by visual domain prompt generation. *arXiv preprint arXiv:2405.02797*, 2024.

David W. Christianson. Structural and chemical biology of terpenoid cyclases. *Chemical Reviews*, 117(17):11570–11648, Sep 2017. ISSN 0009-2665. doi: 10.1021/acs.chemrev.7b00287. URL https://doi.org/10.1021/acs.chemrev.7b00287.

The UniProt Consortium. Uniprot: the universal protein knowledgebase in 2023. *Nucleic acids research*, 51(D1):D523–D531, 2023.

Jacob Devlin. Bert: Pre-training of deep bidirectional transformers for language understanding. *arXiv preprint arXiv:1810.04805*, 2018.

Daniel J Diaz, Chengyue Gong, Jeffrey Ouyang-Zhang, James M Loy, Jordan Wells, David Yang, Andrew D Ellington, Alex Dimakis, and Adam R Klivans. Stability oracle: a structure-based graph-transformer for identifying stabilizing mutations. *BioRxiv*, pp. 2023–05, 2023.

Henry Dieckhaus, Michael Brocidiacono, Nicholas Z Randolph, and Brian Kuhlman. Transfer learning to leverage larger datasets for improved prediction of protein stability changes. *Proceedings of the National Academy of Sciences*, 121(6):e2314853121, 2024.

Janani Durairaj, Andrew M Waterhouse, Toomas Mets, Tetiana Brodiazhenko, Minhal Abdullah, Gabriel Studer, Gerardo Tauriello, Mehmet Akdel, Antonina Andreeva, Alex Bateman, et al. Uncovering new families and folds in the natural protein universe. *Nature*, 622(7983):646–653, 2023.

Oliver Dutton, Sandro Bottaro, Istvan Redl, Michele Invernizzi, Albert Chung, Carlo Fisicaro, Falk Hoffmann, Stefano Ruschetta, Fabio Airoldi, Louie Henderson, et al. Improving inverse folding models at protein stability prediction without additional training or data. *bioRxiv*, pp. 2024–06, 2024.

Ahmed Elnaggar, Hazem Essam, Wafaa Salah-Eldin, Walid Moustafa, Mohamed Elkerdawy, Charlotte Rochereau, and Burkhard Rost. Ankh: Optimized protein language model unlocks general-purpose modelling. *arXiv preprint arXiv:2301.06568*, 2023.

Daniel Esposito, Jochen Weile, Jay Shendure, Lea M Starita, Anthony T Papenfuss, Frederick P Roth, Douglas M Fowler, and Alan F Rubin. Mavedb: an open-source platform to distribute and interpret data from multiplexed assays of variant effect. *Genome biology*, 20:1–11, 2019.

Xiaomin Fang, Fan Wang, Lihang Liu, Jingzhou He, Dayong Lin, Yingfei Xiang, Kunrui Zhu, Xiaonan Zhang, Hua Wu, Hui Li, et al. A method for multiple-sequence-alignment-free protein structure prediction using a protein language model. *Nature Machine Intelligence*, 5(10):1087–1096, 2023.

Tao Feng, Ziqi Gao, Jiaxuan You, Chenyi Zi, Yan Zhou, Chen Zhang, and Jia Li. Deep reinforcement learning for modelling protein complexes. *arXiv preprint arXiv:2405.02299*, 2024.

Noelia Ferruz, Steffen Schmidt, and Birte Höcker. Protgpt2 is a deep unsupervised language model for protein design. *Nature communications*, 13(1):4348, 2022.

Jonathan Frazer, Pascal Notin, Mafalda Dias, Aidan Gomez, Joseph K Min, Kelly Brock, Yarin Gal, and Debora S Marks. Disease variant prediction with deep generative models of evolutionary data. *Nature*, 599(7883):91–95, 2021.

Yossi Gandelsman, Yu Sun, Xinlei Chen, and Alexei Efros. Test-time training with masked autoencoders. *Advances in Neural Information Processing Systems*, 35:29374–29385, 2022.

Yaroslav Ganin and Victor S. Lempitsky. Unsupervised domain adaptation by backpropagation. In Francis R. Bach and David M. Blei (eds.), *Proceedings of the 32nd International Conference on Machine Learning, ICML 2015, Lille, France, 6-11 July 2015*, volume 37 of *JMLR Workshop and Conference Proceedings*, pp. 1180–1189. JMLR.org, 2015. URL `http://proceedings.mlr.press/v37/ganin15.html`.

Jan Gorodkin. Comparing two k-category assignments by a k-category correlation coefficient. *Computational biology and chemistry*, 28(5-6):367–374, 2004.

Xin Gu, Patrick Jouandin, Pranav V. Lalgudi, Rich Binari, Max L. Valenstein, Michael A. Reid, Annamarie E. Allen, Nolan Kamitaki, Jason W. Locasale, Norbert Perrimon, and David M. Sabatini. Sestrin mediates detection of and adaptation to low-leucine diets in drosophila. *Nature*, 608(7921):209–216, Aug 2022. ISSN 1476-4687. doi: 10.1038/s41586-022-04960-2. URL `https://doi.org/10.1038/s41586-022-04960-2`.

Muhammet F. Gulen, Natasha Samson, Alexander Keller, Marius Schwabenland, Chong Liu, Selene Glück, Vivek V. Thacker, Lucie Favre, Bastien Mangeat, Lona J. Kroese, Paul Krimpenfort, Marco Prinz, and Andrea Ablasser. cgas–sting drives ageing-related inflammation and neurodegeneration. *Nature*, 620(7973):374–380, Aug 2023. ISSN 1476-4687. doi: 10.1038/s41586-023-06373-1. URL `https://doi.org/10.1038/s41586-023-06373-1`.

Kathryn H. Gunn and Saskia B. Neher. Structure of dimeric lipoprotein lipase reveals a pore adjacent to the active site. *Nature Communications*, 14(1):2569, May 2023. ISSN 2041-1723. doi: 10.1038/s41467-023-38243-9. URL `https://doi.org/10.1038/s41467-023-38243-9`.

Moritz Hardt and Yu Sun. Test-time training on nearest neighbors for large language models. *arXiv preprint arXiv:2305.18466*, 2023.

Tomas Hayes, Roshan Rao, Halil Akin, Nicholas J Sofroniew, Deniz Oktay, Zeming Lin, Robert Verkuil, Vincent Q Tran, Jonathan Deaton, Marius Wiggert, et al. Simulating 500 million years of evolution with a language model. *bioRxiv*, pp. 2024–07, 2024.

Michael Heinzinger, Konstantin Weissenow, Joaquin Gomez Sanchez, Adrian Henkel, Milot Mirdita, Martin Steinegger, and Burkhard Rost. Bilingual language model for protein sequence and structure. *bioRxiv*, pp. 2023–07, 2023.

Lucas Torroba Hennigen and Yoon Kim. Deriving language models from masked language models. *arXiv preprint arXiv:2305.15501*, 2023.

Thomas A Hopf, John B Ingraham, Frank J Poelwijk, Charlotta PI Schärfe, Michael Springer, Chris Sander, and Debora S Marks. Mutation effects predicted from sequence co-variation. *Nature biotechnology*, 35(2):128–135, 2017.

Gerta Hoxhaj and Brendan D. Manning. The pi3k–akt network at the interface of oncogenic signalling and cancer metabolism. *Nature Reviews Cancer*, 20(2):74–88, Feb 2020. ISSN 1474-1768. doi: 10.1038/s41568-019-0216-7. URL `https://doi.org/10.1038/s41568-019-0216-7`.

Chloe Hsu, Robert Verkuil, Jason Liu, Zeming Lin, Brian Hie, Tom Sercu, Adam Lerer, and Alexander Rives. Learning inverse folding from millions of predicted structures. In *International conference on machine learning*, pp. 8946–8970. PMLR, 2022.

Edward J Hu, Yelong Shen, Phillip Wallis, Zeyuan Allen-Zhu, Yuanzhi Li, Shean Wang, Lu Wang, and Weizhu Chen. Lora: Low-rank adaptation of large language models. *arXiv preprint arXiv:2106.09685*, 2021.

Bowen Jing, Bonnie Berger, and Tommi Jaakkola. Alphafold meets flow matching for generating protein ensembles. *arXiv preprint arXiv:2402.04845*, 2024.

John Jumper, Richard Evans, Alexander Pritzel, Tim Green, Michael Figurnov, Olaf Ronneberger, Kathryn Tunyasuvunakool, Russ Bates, Augustin Žídek, Anna Potapenko, et al. Highly accurate protein structure prediction with alphafold. *nature*, 596(7873):583–589, 2021.

Pranav Kantroo, Gunter Wagner, and Benjamin Machta. Pseudo-perplexity in one fell swoop for protein fitness estimation. *bioRxiv*, pp. 2024–07, 2024.

Neerav Karani, Ertunc Erdil, Krishna Chaitanya, and Ender Konukoglu. Test-time adaptable neural networks for robust medical image segmentation. *Medical Image Analysis*, 68:101907, 2021.

Zuzana Keckesova, Joana Liu Donaher, Jasmine De Cock, Elizaveta Freinkman, Susanne Lingrell, Daniel A. Bachovchin, Brian Bierie, Verena Tischler, Aurelia Noske, Marian C. Okondo, Ferenc Reinhardt, Prathapan Thiru, Todd R. Golub, Jean E. Vance, and Robert A. Weinberg. Lactb is a tumour suppressor that modulates lipid metabolism and cell state. *Nature*, 543(7647):681–686, Mar 2017. ISSN 1476-4687. doi: 10.1038/nature21408. URL https://doi.org/10.1038/nature21408.

Diederik P. Kingma and Jimmy Ba. Adam: A method for stochastic optimization. In Yoshua Bengio and Yann LeCun (eds.), *3rd International Conference on Learning Representations, ICLR 2015, San Diego, CA, USA, May 7-9, 2015, Conference Track Proceedings*, 2015. URL http://arxiv.org/abs/1412.6980.

Andrew Kirjner, Jason Yim, Raman Samusevich, Shahar Bracha, Tommi S Jaakkola, Regina Barzilay, and Ila R Fiete. Improving protein optimization with smoothed fitness landscapes. In *The Twelfth International Conference on Learning Representations*, 2023.

Petr Kouba, Pavel Kohout, Faraneh Haddadi, Anton Bushuiev, Raman Samusevich, Jiri Sedlar, Jiri Damborsky, Tomas Pluskal, Josef Sivic, and Stanislav Mazurenko. Machine learning-guided protein engineering. *ACS catalysis*, 13(21):13863–13895, 2023.

Andriy Kryshtafovych, Torsten Schwede, Maya Topf, Krzysztof Fidelis, and John Moult. Critical assessment of methods of protein structure prediction (casp)—round xv. *Proteins: Structure, Function, and Bioinformatics*, 91(12):1539–1549, 2023. doi: https://doi.org/10.1002/prot.26617. URL https://onlinelibrary.wiley.com/doi/abs/10.1002/prot.26617.

Elodie Laine, Yasaman Karami, and Alessandra Carbone. Gemme: a simple and fast global epistatic model predicting mutational effects. *Molecular biology and evolution*, 36(11):2604–2619, 2019.

Zeming Lin, Halil Akin, Roshan Rao, Brian Hie, Zhongkai Zhu, Wenting Lu, Nikita Smetanin, Robert Verkuil, Ori Kabeli, Yaniv Shmueli, Allan dos Santos Costa, Maryam Fazel-Zarandi, Tom Sercu, Salvatore Candido, and Alexander Rives. Evolutionary-scale prediction of atomic-level protein structure with a language model. *Science*, 379(6637):1123–1130, 2023. doi: 10.1126/science.ade2574. URL https://www.science.org/doi/abs/10.1126/science.ade2574.

Yuejiang Liu, Parth Kothari, Bastien van Delft, Baptiste Bellot-Gurlet, Taylor Mordan, and Alexandre Alahi. TTT++: when does self-supervised test-time training fail or thrive? In Marc'Aurelio Ranzato, Alina Beygelzimer, Yann N. Dauphin, Percy Liang, and Jennifer Wortman Vaughan (eds.), *Advances in Neural Information Processing Systems 34: Annual Conference on Neural Information Processing Systems 2021, NeurIPS 2021, December 6-14, 2021, virtual*, pp. 21808–21820, 2021. URL https://proceedings.neurips.cc/paper/2021/hash/b618c3210e934362ac261db280128c22-Abstract.html.

Ilya Loshchilov and Frank Hutter. Decoupled weight decay regularization. In *7th International Conference on Learning Representations, ICLR 2019, New Orleans, LA, USA, May 6-9, 2019*. OpenReview.net, 2019. URL https://openreview.net/forum?id=Bkg6RiCqY7.

Ali Madani, Ben Krause, Eric R Greene, Subu Subramanian, Benjamin P Mohr, James M Holton, Jose Luis Olmos, Caiming Xiong, Zachary Z Sun, Richard Socher, et al. Large language models generate functional protein sequences across diverse families. *Nature Biotechnology*, 41(8): 1099–1106, 2023.

Valerio Mariani, Marco Biasini, Alessandro Barbato, and Torsten Schwede. lddt: a local superposition-free score for comparing protein structures and models using distance difference tests. *Bioinformatics*, 29(21):2722–2728, 2013.

Joshua Meier, Roshan Rao, Robert Verkuil, Jason Liu, Tom Sercu, and Alex Rives. Language models enable zero-shot prediction of the effects of mutations on protein function. *Advances in neural information processing systems*, 34:29287–29303, 2021.

Peter Mikhael, Itamar Chinn, and Regina Barzilay. Clipzyme: Reaction-conditioned virtual screening of enzymes. In *Forty-first International Conference on Machine Learning, ICML 2024, Vienna, Austria, July 21-27, 2024*. OpenReview.net, 2024. URL `https://openreview.net/forum?id=0mYAK6Yhhm`.

Amir Motmaen, Justas Dauparas, Minkyung Baek, Mohamad H Abedi, David Baker, and Philip Bradley. Peptide-binding specificity prediction using fine-tuned protein structure prediction networks. *Proceedings of the National Academy of Sciences*, 120(9):e2216697120, 2023.

Pascal Notin, Mafalda Dias, Jonathan Frazer, Javier Marchena-Hurtado, Aidan N Gomez, Debora Marks, and Yarin Gal. Tranception: protein fitness prediction with autoregressive transformers and inference-time retrieval. In *International Conference on Machine Learning*, pp. 16990–17017. PMLR, 2022a.

Pascal Notin, Lood Van Niekerk, Aaron W Kollasch, Daniel Ritter, Yarin Gal, and Debora S Marks. Trancepteve: Combining family-specific and family-agnostic models of protein sequences for improved fitness prediction. *bioRxiv*, pp. 2022–12, 2022b.

Pascal Notin, Aaron Kollasch, Daniel Ritter, Lood Van Niekerk, Steffanie Paul, Han Spinner, Nathan Rollins, Ada Shaw, Rose Orenbuch, Ruben Weitzman, et al. Proteingym: Large-scale benchmarks for protein fitness prediction and design. *Advances in Neural Information Processing Systems*, 36, 2024.

Dong oh Seo, David O'Donnell, Nimansha Jain, Jason D. Ulrich, Jasmin Herz, Yuhao Li, Mackenzie Lemieux, Jiye Cheng, Hao Hu, Javier R. Serrano, Xin Bao, Emily Franke, Maria Karlsson, Martin Meier, Su Deng, Chandani Desai, Hemraj Dodiya, Janaki Lelwala-Guruge, Scott A. Handley, Jonathan Kipnis, Sangram S. Sisodia, Jeffrey I. Gordon, and David M. Holtzman. Apoe isoform– and microbiota-dependent progression of neurodegeneration in a mouse model of tauopathy. *Science*, 379(6628):eadd1236, 2023. doi: 10.1126/science.add1236. URL `https://www.science.org/doi/abs/10.1126/science.add1236`.

Andrei Papkou, Lucia Garcia-Pastor, José Antonio Escudero, and Andreas Wagner. A rugged yet easily navigable fitness landscape. *Science*, 382(6673):eadh3860, 2023. doi: 10.1126/science.adh3860. URL `https://www.science.org/doi/abs/10.1126/science.adh3860`.

Predrag Radivojac and et al. A large-scale evaluation of computational protein function prediction. *Nature Methods*, 10(3):221–227, Mar 2013. ISSN 1548-7105. doi: 10.1038/nmeth.2340. URL `https://doi.org/10.1038/nmeth.2340`.

Roshan Rao, Nicholas Bhattacharya, Neil Thomas, Yan Duan, Peter Chen, John Canny, Pieter Abbeel, and Yun Song. Evaluating protein transfer learning with tape. *Advances in neural information processing systems*, 32, 2019.

Roshan Rao, Joshua Meier, Tom Sercu, Sergey Ovchinnikov, and Alexander Rives. Transformer protein language models are unsupervised structure learners. *Biorxiv*, pp. 2020–12, 2020.

Roshan M Rao, Jason Liu, Robert Verkuil, Joshua Meier, John Canny, Pieter Abbeel, Tom Sercu, and Alexander Rives. Msa transformer. In *International Conference on Machine Learning*, pp. 8844–8856. PMLR, 2021.

Ali Razavi, Aäron van den Oord, and Oriol Vinyals. Generating diverse high-fidelity images with VQ-VAE-2. In Hanna M. Wallach, Hugo Larochelle, Alina Beygelzimer, Florence d'Alché-Buc, Emily B. Fox, and Roman Garnett (eds.), *Advances in Neural Information Processing Systems 32: Annual Conference on Neural Information Processing Systems 2019, NeurIPS 2019, December 8-14, 2019, Vancouver, BC, Canada*, pp. 14837–14847, 2019. URL `https://proceedings.neurips.cc/paper/2019/hash/5f8e2fa1718d1bbcadf1cd9c7a54fb8c-Abstract.html`.

Alexander Rives, Joshua Meier, Tom Sercu, Siddharth Goyal, Zeming Lin, Jason Liu, Demi Guo, Myle Ott, C Lawrence Zitnick, Jerry Ma, et al. Biological structure and function emerge from scaling unsupervised learning to 250 million protein sequences. *Proceedings of the National Academy of Sciences*, 118(15):e2016239118, 2021.

Xavier Robin, Juergen Haas, Rafal Gumienny, Anna Smolinski, Gerardo Tauriello, and Torsten Schwede. Continuous automated model evaluation (cameo)—perspectives on the future of fully automated evaluation of structure prediction methods. *Proteins: Structure, Function, and Bioinformatics*, 89(12):1977–1986, 2021.

Sebastian Ruder. An overview of gradient descent optimization algorithms. *arXiv preprint arXiv:1609.04747*, 2016.

Nataniel Ruiz, Yuanzhen Li, Varun Jampani, Yael Pritch, Michael Rubinstein, and Kfir Aberman. Dreambooth: Fine tuning text-to-image diffusion models for subject-driven generation. In *Proceedings of the IEEE/CVF conference on computer vision and pattern recognition*, pp. 22500–22510, 2023.

Julian Salazar, Davis Liang, Toan Q Nguyen, and Katrin Kirchhoff. Masked language model scoring. *arXiv preprint arXiv:1910.14659*, 2019.

Raman Samusevich, Téo Hebra, Roman Bushuiev, Anton Bushuiev, Tereza Čalounová, Helena Smrčková, Ratthachat Chatpatanasiri, Jonáš Kulhánek, Milana Perković, Martin Engst, Adéla Tajovská, Josef Sivic, and Tomáš Pluskal. Highly accurate discovery of terpene synthases powered by machine learning reveals functional terpene cyclization in archaea. *bioRxiv*, 2024. doi: 10.1101/2024.01.29.577750. URL https://www.biorxiv.org/content/early/2024/04/25/2024.01.29.577750.

Nicolae Sapoval, Amirali Aghazadeh, Michael G. Nute, Dinler A. Antunes, Advait Balaji, Richard Baraniuk, C. J. Barberan, Ruth Dannenfelser, Chen Dun, Mohammadamin Edrisi, R. A. Leo Elworth, Bryce Kille, Anastasios Kyrillidis, Luay Nakhleh, Cameron R. Wolfe, Zhi Yan, Vicky Yao, and Todd J. Treangen. Current progress and open challenges for applying deep learning across the biosciences. *Nature Communications*, 13(1):1728, Apr 2022. ISSN 2041-1723. doi: 10.1038/s41467-022-29268-7. URL https://doi.org/10.1038/s41467-022-29268-7.

Emre Sevgen, Joshua Moller, Adrian Lange, John Parker, Sean Quigley, Jeff Mayer, Poonam Srivastava, Sitaram Gayatri, David Hosfield, Maria Korshunova, et al. Prot-vae: protein transformer variational autoencoder for functional protein design. *bioRxiv*, pp. 2023–01, 2023.

Raghav Shroff, Austin W Cole, Daniel J Diaz, Barrett R Morrow, Isaac Donnell, Ankur Annapareddy, Jimmy Gollihar, Andrew D Ellington, and Ross Thyer. Discovery of novel gain-of-function mutations guided by structure-based deep learning. *ACS synthetic biology*, 9(11):2927–2935, 2020.

Yidong Song, Qianmu Yuan, Sheng Chen, Yuansong Zeng, Huiying Zhao, and Yuedong Yang. Accurately predicting enzyme functions through geometric graph learning on esmfold-predicted structures. *Nature Communications*, 15(1):8180, 2024.

Hannes Stärk, Christian Dallago, Michael Heinzinger, and Burkhard Rost. Light attention predicts protein location from the language of life. *Bioinformatics Advances*, 1(1):vbab035, 11 2021. ISSN 2635-0041. doi: 10.1093/bioadv/vbab035. URL https://doi.org/10.1093/bioadv/vbab035.

Jin Su, Chenchen Han, Yuyang Zhou, Junjie Shan, Xibin Zhou, and Fajie Yuan. Saprot: Protein language modeling with structure-aware vocabulary. *bioRxiv*, pp. 2023–10, 2023.

Sriram Subramaniam and Gerard J. Kleywegt. A paradigm shift in structural biology. *Nature Methods*, 19(1):20–23, Jan 2022. ISSN 1548-7105. doi: 10.1038/s41592-021-01361-7. URL https://doi.org/10.1038/s41592-021-01361-7.

Yu Sun, Xiaolong Wang, Zhuang Liu, John Miller, Alexei Efros, and Moritz Hardt. Test-time training with self-supervision for generalization under distribution shifts. In *International conference on machine learning*, pp. 9229–9248. PMLR, 2020.

Nataša Tagasovska, Ji Won Park, Matthieu Kirchmeyer, Nathan C Frey, Andrew Martin Watkins, Aya Abdelsalam Ismail, Arian Rokkum Jamasb, Edith Lee, Tyler Bryson, Stephen Ra, et al. Antibody domainbed: Out-of-distribution generalization in therapeutic protein design. *arXiv preprint arXiv:2407.21028*, 2024.

Kotaro Tsuboyama, Justas Dauparas, Jonathan Chen, Elodie Laine, Yasser Mohseni Behbahani, Jonathan J Weinstein, Niall M Mangan, Sergey Ovchinnikov, and Gabriel J Rocklin. Mega-scale experimental analysis of protein folding stability in biology and design. *Nature*, 620(7973): 434–444, 2023.

Mike Tyers and Matthias Mann. From genomics to proteomics. *Nature*, 422(6928):193–197, Mar 2003. ISSN 1476-4687. doi: 10.1038/nature01510. URL https://doi.org/10.1038/nature01510.

Michel van Kempen, Stephanie S Kim, Charlotte Tumescheit, Milot Mirdita, Cameron LM Gilchrist, Johannes Söding, and Martin Steinegger. Foldseek: fast and accurate protein structure search. *Biorxiv*, pp. 2022–02, 2022.

Mihaly Varadi, Stephen Anyango, Mandar Deshpande, Sreenath Nair, Cindy Natassia, Galabina Yordanova, David Yuan, Oana Stroe, Gemma Wood, Agata Laydon, et al. Alphafold protein structure database: massively expanding the structural coverage of protein-sequence space with high-accuracy models. *Nucleic acids research*, 50(D1):D439–D444, 2022.

A Vaswani. Attention is all you need. *Advances in Neural Information Processing Systems*, 2017.

Renhao Wang, Yu Sun, Yossi Gandelsman, Xinlei Chen, Alexei A Efros, and Xiaolong Wang. Test-time training on video streams. *arXiv preprint arXiv:2307.05014*, 2023.

Joseph L Watson, David Juergens, Nathaniel R Bennett, Brian L Trippe, Jason Yim, Helen E Eisenach, Woody Ahern, Andrew J Borst, Robert J Ragotte, Lukas F Milles, et al. De novo design of protein structure and function with rfdiffusion. *Nature*, 620(7976):1089–1100, 2023.

Zehao Xiao, Xiantong Zhen, Ling Shao, and Cees GM Snoek. Learning to generalize across domains on single test samples. *arXiv preprint arXiv:2202.08045*, 2022.

Jason Yang, Francesca-Zhoufan Li, and Frances H. Arnold. Opportunities and challenges for machine learning-assisted enzyme engineering. *ACS Central Science*, 10(2):226–241, Feb 2024. ISSN 2374-7943. doi: 10.1021/acscentsci.3c01275. URL https://doi.org/10.1021/acscentsci.3c01275.

Tianhao Yu, Haiyang Cui, Jianan Canal Li, Yunan Luo, Guangde Jiang, and Huimin Zhao. Enzyme function prediction using contrastive learning. *Science*, 379(6639):1358–1363, 2023. doi: 10.1126/science.adf2465. URL https://www.science.org/doi/abs/10.1126/science.adf2465.

Marvin Zhang, Henrik Marklund, Nikita Dhawan, Abhishek Gupta, Sergey Levine, and Chelsea Finn. Adaptive risk minimization: Learning to adapt to domain shift. In Marc'Aurelio Ranzato, Alina Beygelzimer, Yann N. Dauphin, Percy Liang, and Jennifer Wortman Vaughan (eds.), *Advances in Neural Information Processing Systems 34: Annual Conference on Neural Information Processing Systems 2021, NeurIPS 2021, December 6-14, 2021, virtual*, pp. 23664–23678, 2021. URL https://proceedings.neurips.cc/paper/2021/hash/c705112d1ec18b97acac7e2d63973424-Abstract.html.

Yang Zhang and Jeffrey Skolnick. Scoring function for automated assessment of protein structure template quality. *Proteins: Structure, Function, and Bioinformatics*, 57(4):702–710, 2004.

Hao Zhao, Yuejiang Liu, Alexandre Alahi, and Tao Lin. On pitfalls of test-time adaptation. In Andreas Krause, Emma Brunskill, Kyunghyun Cho, Barbara Engelhardt, Sivan Sabato, and Jonathan Scarlett (eds.), *International Conference on Machine Learning, ICML 2023, 23-29 July 2023, Honolulu, Hawaii, USA*, volume 202 of *Proceedings of Machine Learning Research*, pp. 42058–42080. PMLR, 2023. URL https://proceedings.mlr.press/v202/zhao23d.html.

APPENDIX

In Appendix A, we provide further details on the experimental setup, including comprehensive descriptions of the models, datasets, and metrics used. Next, in Appendix B, we present additional results and their analysis. We discuss the distribution of TTT effects and demonstrate that TTT primarily improves performance on challenging targets. We also explore the impact of hyperparameters by showing the performance on validation sets.

A   EXPERIMENTAL DETAILS

In this section, we describe the experimental details for the three downstream tasks considered in this work: protein fitness prediction (Appendix A.1), protein structure prediction (Appendix A.2), and protein function prediction (Appendix A.3). Each subsection describes the application of test-time training (TTT) to the respective models, along with details on the datasets, metrics, and models. Table 4 additionally summarizes the hyperparameters used for the application of TTT to individual models.

A.1   PROTEIN FITNESS PREDICTION

A.1.1   DATASETS

ProteinGym.   ProteinGym is the standard benchmark for protein fitness prediction (Notin et al., 2024). The latest, second version of the dataset includes 217 deep mutation scanning experiments (DMSs) across different proteins. In total, the dataset contains 2.5 mutants with annotated ground-truth fitness. Since ProteinGym does not contain a data split for the zero-shot setup, employed in this work, we use the whole dataset as the test set.

MaveDB dataset.   To establish a validation set disjoint from ProteinGym (Notin et al., 2024), we mined MaveDB[3] (Esposito et al., 2019). As of August 1, 2024, the database contains 1178 Multiplexed Assays of Variant Effects (MAVEs), where each assay corresponds to a single protein, measuring the experimental fitness of its variants. We applied quality control filters to remove potentially noisy data. Specifically, we ensured that the UniProt identifier (Consortium, 2023) is valid and has a predicted structure available in the AlphaFold DB (Varadi et al., 2022). We also excluded assays with fewer than 100 variants, as well as those where at least one mutation had a wrongly annotated wild type or where most mutations failed during parsing. Additionally, to ensure no overlap between datasets, we removed any assays whose UniProt identifier matched with those in ProteinGym, ensuring that the validation and test sets contain different proteins.

The described methodology resulted in the MaveDB dataset comprising 676 assays (out of 1178 in the entire MaveDB) with experimental fitness annotations. This corresponds to 483 unique protein sequences and 867 thousand mutations in total. The large size of the dataset, despite the comprehensiveness of ProteinGym containing 217 assays, can be attributed to the fact that many assays in MaveDB were released after the ProteinGym construction (Figure 6A). To ensure the quality of the constructed MaveDB dataset, we validated that representative baselines from ProteinGym generalize to the new assays, following a similar distribution of predictions (Figure 6B,C). Finally, for efficiently tuning hyper-parameters for fitness prediction models we sampled 50 random proteins (Figure 6D), corresponding to 83 assays and collectively 134 thousand variants.

A.1.2   METRICS

Protein fitness labels are not standardized and can vary across different proteins. Nevertheless, the ranking of mutations for a single protein, as defined by fitness labels, can be used to assess the mutation scoring capabilities of machine learning models. As a result, Spearman correlation is a standard metric for evaluation.

Spearman by phenotype.   When computing Spearman correlations, we follow the evaluation protocol proposed in ProteinGym (Notin et al., 2024). First, for each protein, we compute Spearman

---

[3]https://www.mavedb.org
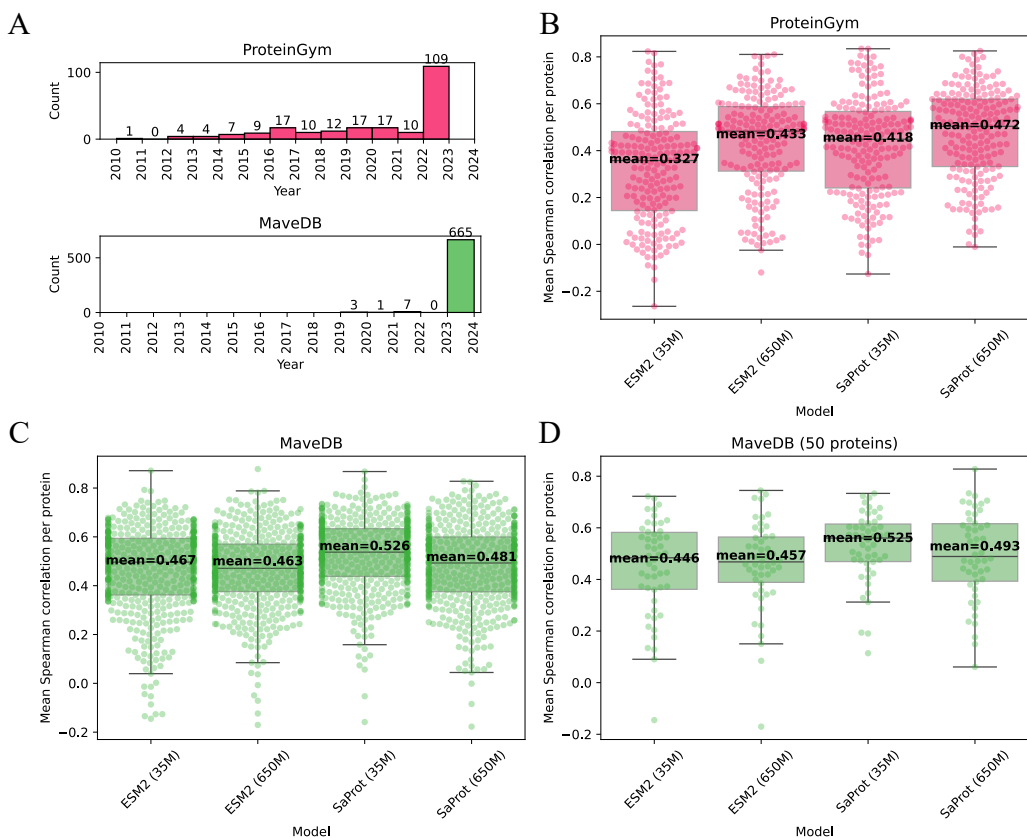
Figure 6: **Comparison of the standard ProteinGym dataset with the MaveDB dataset constructed in this work**. A) MaveDB, mined from Esposito et al. (2019), includes novel assays even after filtering to ensure distinct proteins from the comprehensive ProteinGym dataset. This is largely because most MaveDB assays post-filtering date to 2024, whereas the latest assays in ProteinGym date to 2023. B, C, D) MaveDB is of sufficient quality for model evaluation. Representative baselines, ESM2 and SaProt with both 35 million and 650 million parameters, evaluated on ProteinGym generalize effectively to MaveDB, following a similar distribution of predictions. Panel D illustrates the random subset of 50 proteins used for hyperparameter tuning for fitness prediction. Each point in the plots represents one protein and shows the Spearman correlation averaged across all assays corresponding to the protein (typically one assay per protein). The box plots standardly depict quartiles, medians, and outliers.

correlation scores between the predicted ranks of mutations and their corresponding labels. Then, we average the scores across five categories of assayed phenotypes, measuring the effects of introduced mutations: protein catalytic activity ("Activity"), binding affinity to a target ("Binding"), protein expression levels in a cell ("Expression"), organism growth rate ("Organismal Fitness"), and protein thermostability ("Stability").

Avg. Spearman.   We refer to the mean score across the five phenotype categories as "Avg. Spearman". We report the "Avg. Spearman" metric as the mean and standard deviation across five random seeds (Table 1, Table 5).

Spearman by MSA Depth.   Following (Notin et al., 2024), we split the performance by the depth of available multiple sequence alignment (MSA), i.e., the number of homologous sequences available, as provided in ProteinGym: "Low depth", "Medium depth", and "High depth", and report the Spearman correlation for each subset individually (Table 6). Specifically, the MSA depth categories in ProteinGym are determined using the following thresholds from Hopf et al. (2017): "Low" is

defined as $N_{eff}/L < 1$, "Medium" as $1 < N_{eff}/L < 100$, and "High" as $N_{eff}/L > 100$, where N_{eff} represents the normalized number of effective sequences in the MSA, and L is the sequence length covered in the MSA.

A.1.3 MODELS

ESM2. The ESM2 model is a bidirectional, BERT-like (Devlin, 2018) transformer trained on millions of protein sequences using masked modeling (Lin et al., 2023). The goal of protein fitness prediction is to predict the effects of mutations, and protein language models are often adapted to this task using zero-shot transfer via log odds ratio (Notin et al., 2024; Meier et al., 2021). Specifically, for a given single- or multi-point mutation, where certain amino acids T are substituted from x_i to x_i^m for each $i \in T$, the fitness prediction via the log odds ratio is defined as:

$$\sum_{i \in T} \log p(x_i^m | x_{\setminus i}) - \log p(x_i | x_{\setminus i}), \tag{3}$$

where the sum iterates over mutated positions $i \in T$ with $p(x_i^m | x_{\setminus i})$ and $p(x_i | x_{\setminus i})$ denoting the predicted probabilities of the mutated amino acid and the original one (i.e., wild type), respectively. The conditionals $x_{\setminus i}$ indicate that the input sequence to the model has the position i masked. In this setup, the native (unmutated) sequence, where $T = \emptyset$, has a predicted fitness of 0. Mutations with negative values represent favorable mutations, while positive values correspond to disruptive mutations. We follow the ProteinGym benchmark[4] and use this formula (Notin et al., 2024) to evaluate the fitness prediction capabilities of ESM2. We use the implementation of ESM2 from ProteinGym.

ESM2 + TTT. ESM2 can be straightforwardly enhanced with test-time training. Specifically, we treat the transformer encoder as the backbone f, and the language modeling head, which projects token embeddings to amino acid probabilities, as the pre-training head g. The log odds ratio given by Equation (3) serves as the task-specific head h, which in this case involves the pre-training head g that predicts log probabilities. Overall, we apply TTT to the pre-trained ESM2 model and, after a pre-defined number of self-supervised fine-tuning steps, score mutations using Equation (3). During TTT we fine-tune all parameters in $g \circ f$ end-to-end except for token and position embeddings.

SaProt. We also experiment with the state-of-the-art fitness prediction model, SaProt (Su et al., 2023). SaProt builds off the ESM2 model but incorporates structural information from predicted protein structures. Specifically, SaProt uses the same transformer architecture but expands its vocabulary by combining the 20 standard amino acid tokens with 20 structural tokens from the 3Di vocabulary, increasing the total alphabet size to 400. The 3Di tokens capture the geometry of the protein backbone and are generated using VQ-VAE (Razavi et al., 2019), which projects continuous geometric information into discrete tokens and was trained as part of the Foldseek method (van Kempen et al., 2022).

Since SaProt is also a protein language model, it also uses Equation (3) to score variants. However, please note that SaProt, as implemented in ProteinGym (Notin et al., 2024), uses a slightly different version of the log odds ratio. In SaProt, the conditions in the log probabilities in Equation (3) are replaced with $x_{\setminus T}$ instead of $x_{\setminus i}$, not assuming the independence of substitutions. During TTT, we only mask sequential information and leave the structural part of the tokens unchanged, reflecting the original pre-training setup. We use the implementation of SaProt from ProteinGym[4].

SaProt + TTT. Since the architecture of SaProt is based on ESM2, the TTT components f, g, and h remain the same. It means that test-time training can be applied to the model in the same way as in the case of ESM2 + TTT discussed above.

A.2 PROTEIN STRUCTURE PREDICTION

A.2.1 DATASETS

CAMEO dataset. To evaluate the capabilities of TTT on protein folding, we employ the CAMEO validation and test sets as described in Lin et al. (2023). Specifically, the validation set was obtained

---

[4]`https://github.com/OATML-Markslab/ProteinGym`

by querying the CAMEO (Continuous Automated Model Evaluation) web server[5] (Robin et al., 2021) for entries between August 2021 and January 2022, while the CAMEO test set consists of entries from April 1, 2022, to June 25, 2022. Most of the entries in the CAMEO sets are predicted with high accuracy and confidence (Lin et al., 2023). Therefore, we subselected the challenging validation and test sets where TTT is relevant.

Specifically, we applied two criteria: (1) preserving entries with ESMFold pLDDT scores below 70 to filter out high-confidence predictions (Jumper et al., 2021), and (2) selecting entries with ESM2 perplexity scores greater than or equal to 6, ensuring that the predictions are challenging due to poor sequence understanding rather than other factors. Additionally, most structures with perplexity scores below 6 are already associated with high-confidence predictions (Figure S5 in Lin et al. (2023)). After filtering, the resulting challenging validation and test sets consist of 27 (out of 378) and 18 (out of 194) targets, respectively. The vast majority of the remaining structures have accurate ESMFold structure predictions.

A.2.2 METRICS

To assess the quality of the predicted protein structures with respect to the ground truth structures, we use two standard metrics averaged across the test dataset: TM-score (Zhang & Skolnick, 2004) and LDDT (Mariani et al., 2013).

TM-score. The TM-score (Template Modeling score) is a metric used to assess the quality of the global 3D alignment between the predicted and target protein structures. It evaluates the structural similarity by comparing the distance between corresponding residues after superposition. The TM-score ranges from 0 to 1, where higher values indicate better alignment.

LDDT. The Local Distance Difference Test (LDDT) is an alignment-free metric used to assess the accuracy of predicted protein structures. Unlike global metrics, LDDT focuses on local structural differences by measuring the deviation in distances between atom pairs in the predicted structure compared to the target structure. It is particularly useful for evaluating the accuracy of local regions, such as secondary structure elements. LDDT scores range from 0 to 100, with higher values indicating better local structural agreement.

A.2.3 MODELS

ESMFold. The ESMFold architecture comprises two key components: a protein language model, ESM2, which, given a protein sequence, generates embeddings for individual amino acids, and a folding block that, using these embeddings and the sequence, predicts the protein 3D structure along with per-amino-acid confidence scores, known as pLDDT scores. In our experiments, we use the `esmfold_v0` model from the publicly available ESMFold checkpoints[6]. Please note that we use `esmfold_v0` and not `esmfold_v1` to avoid data leakage with respect to the CAMEO test set.

ESMFold + TTT. Since ESM2 backbone of ESMFold was pre-trained in a self-supervised masked modeling regime, the application of TTT to ESMFold is straightforward. We treat ESM2 as the backbone f, the language modeling head predicting amino acid classes from their embeddings as the self-supervised head g, and the folding trunk along with the structure modules as the downstream task head h. After each TTT step, we run $h \circ f$ to compute the pLDDT scores, which allows us to estimate the optimal number of TTT steps for each protein based on the highest pLDDT score.

Since the backbone f is given by the ESM2 model containing 3 billion parameters, we apply LoRA (Hu et al., 2021) to all matrices involved in self-attention. This enables fine-tuning ESMFold + TTT on a single GPU.

ESMFold + ME. Since ESMFold is a regression model, it only predicts one solution and does not have a straightforward mechanism of sampling multiple structure predictions. Nevertheless, the authors of ESMFold propose a way to sample multiple candidates (Section A.3.2 in Lin et al. (2023)).

---

[5]https://www.cameo3d.org/modeling
[6]https://github.com/facebookresearch/esm/blob/main/esm/esmfold/v1/pretrained.py

To sample more solutions, the masking prediction (ME) method randomly masks 15% (same ratio as during masked language modeling pre-training) of the amino acids embeddings before passing them to the structure prediction block. Selecting the solution with the highest pLDDT may lead to improved predicted structure. Since sampling multiple solutions with ESMFold + ME and selecting the best one via pLDDT is analogous to ESMFold + TTT, we employ the former as a baseline, running the method for the same number of step.

ESM3. Unlike ESMFold, ESM3 is a fully multiple-track, BERT-like model (Devlin, 2018), pre-trained to unmask both protein sequence and structure tokens simultaneously (along with the function tokens). The structure tokens in ESM3 are generated via a separately pre-trained VQ-VAE (Razavi et al., 2019) operating on the protein geometry. In our experiments, we use the smallest, publicly available version of the ESM3 model (`ESM3_sm_open_v0`)[7].

ESM3 + TTT. We treat the transformer encoder of ESM3 as f, the language modeling head decoding amino acid classes as g, and the VQ-VAE decoder, which maps structure tokens to the 3D protein structure, as h. During the TTT steps, we train the model to unmask a protein sequence while keeping the structural track fully padded. During the inference, we provide the model with a protein sequence and run it to unmask the structural tokens, which are subsequently decoded with the VQ-VAE decoder. After each TTT step, we run $h \circ f$ to compute the pLDDT scores, which allows us to estimate the optimal number of TTT steps for each protein based on the highest pLDDT score. We choose the optimal hyperparameters by maximizing the difference in TM-score after and before applying TTT across the validation dataset.

Figure 7: Average running time of ESM3 + TTT (50 steps) on the CAMEO validation set using a single NVIDIA A100 GPU.

Despite the fact that the model contains 1.4 billion parameters, even without using LoRA, ESM3 + TTT can be fine-tuned on a single NVIDIA A100 GPU. Therefore, we do not employ LoRA for fine-tuning ESM3. Figure 7 shows that ESM3 + TTT can be loaded in VRAM and run for 50 steps in just 10 seconds, with an additional 10 seconds overhead for pLDDT estimation. For comparison, the base ESM3 model can be run on the same hardware in 1 second.
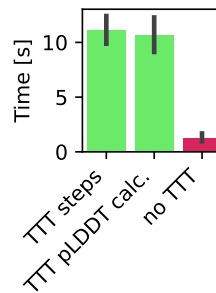
ESM3 + CoT. To improve the generalization and protein-specific performance of ESM3, the original ESM3 paper employs a chain of thought (CoT) procedure. The procedure unfolds in n steps as follows. At each step, $1/n$ of the masked tokens with the lowest entropy after softmax on logits are unmasked. Then, the partially unmasked sequence is fed back into the model, and the process repeats until the entire sequence is unmasked. In our experiments, we set $n = 8$, which is the default value provided in the official GitHub repository.

A.3 PROTEIN FUNCTION PREDICTION

A.3.1 DATASETS

TPS dataset. For the evaluation of terpene substrate classification, we use the largest available dataset of characterized TPS enzymes from Samusevich et al. (2024) and repurpose the original 5-fold cross-validation schema. We focus on the most challenging TPS sequences, defined as those predicted by the TPS detector, proposed by the dataset authors, with confidence scores below 0.8. This filtering results in 104, 98, 113, 100, 97 examples in the individual folds.

setHard. For the test evaluation of subcellular location prediction, we use the setHard dataset constructed by Stärk et al. (2021). The dataset was redundancy-reduced, both within itself and relative to all proteins in DeepLoc (Almagro Armenteros et al. (2017); next paragraph), a standard dataset used for training and validating machine learning models. The setHard dataset contains 490 protein sequences, each annotated with one of ten subcellular location classes, such as "Cytoplasm" or "Nucleus". Since we use ESM-1b (Rives et al., 2021) in our experiments with the dataset, we

---

[7]https://github.com/evolutionaryscale/esm

further filter the data to 432 sequences that do not exceed a length of 1022 amino acids. This step, consistent with Stärk et al. (2021), ensures that ESM-1b can generate embeddings for all proteins.

DeepLoc. For hyperparameter tuning in the subcellular location prediction task, we use the test set from the DeepLoc dataset (Almagro Armenteros et al., 2017). Similar to setHard, DeepLoc assigns labels from one of ten subcellular location classes. The dataset contains 2768 proteins, which we further filter to 2457 sequences that do not exceed a length of 1022 amino acids, ensuring compatibility with the embedding capabilities of ESM-1b. Since setHard was constructed to be independent of DeepLoc, setHard provides a leakage-free source of data for validation.

A.3.2 METRICS

mAP, AUROC. The TPS substrate prediction problem is a 12-class multi-label classification task over possible TPS substrates. Therefore, we assess the quality of the predictions using standard multi-label classification metrics such as mean average precision (mAP) and area under the receiver operating characteristic curve (AUROC) averaged across individual classes. These metrics were used in the original TerpeneMiner paper (Samusevich et al., 2024). We report the performance by averaging the metric values concatenated across all validation folds from the 5-fold cross-validation schema.

Accuracy, MCC, F1-score. To evaluate the performance of subcellular location prediction methods, we use standard classification metrics as employed in Stärk et al. (2021). Accuracy standardly measures the ratio of correctly classified proteins, while Matthew's correlation coefficient for multiple classes (MCC) serves as an alternative to the Pearson correlation coefficient for classification tasks (Gorodkin, 2004). The F1-score, the harmonic mean of precision and recall, evaluates performance from a retrieval perspective, balancing the trade-off between false positives and false negatives.

A.3.3 MODELS

TerpeneMiner. TerpeneMiner is a state-of-the-art method for the classification of terpene synthase (TPS) substrates (Samusevich et al., 2024). The model consists of two parallel tracks. Given a protein sequence, TerpeneMiner first computes its ESM-1v embedding (Meier et al., 2021) and a vector of similarities to the functional domains of proteins from the training dataset, based on unsupervised domain segmentation of AlphaFold2-predicted structures (Jumper et al., 2021). The ESM-1v embedding and the similarity vector are then concatenated and processed by a separately trained random forest, which predicts TPS substrate class probabilities.

In our experiments, we use the "PLM only" version of the model, which leverages only ESM-1v embeddings (PLM stands for protein language model). This version exhibits a minor performance decrease compared to the full model but exactly follows a Y-shaped architecture, allowing us to validate the effectiveness of test-time training for predicting TPS substrates. We use the implementation of TerpeneMiner available at the official GitHub page [8].

TerpeneMiner + TTT. When applying TTT to TerpeneMiner, we treat the frozen ESM-1v model as a backbone f, its language modeling head as a self-supervised head g, and the random forest classifying TPS substrates as a downstream supervised head h.

Light Attention. We use Light attention (Stärk et al., 2021) as a representative baseline for subcellular location prediction. Light attention leverages protein embeddings from a language model, which in our case is ESM-1b (Rives et al., 2021). The model processes per-residue embeddings via a softmax-weighted aggregation mechanism, referred to as light attention, which operates with linear complexity relative to sequence length and enables richer aggregation of per-residue information, as opposed to standard mean pooling. We re-train the model using ESM-1b embeddings on the DeepLoc dataset (Almagro Armenteros et al., 2017) using the code from the official GitHub page[9].

---

[8] https://github.com/pluskal-lab/TerpeneMiner
[9] https://github.com/HannesStark/protein-localization

Table 4: **Hyperparameters used for adapting TTT to individual models.** The optimal hyperparameters were estimated using validation datasets corresponding to each of the considered tasks: *Fitness prediction*, *Structure prediction*, and *Function prediction*. Comma-separated lists show the values used for hyperparameter grid search, while the final values selected for computing the test results are highlighted in **bold**. Low-rank adaptation (LoRA) was only used with ESMFold, containing 3 billion parameters in the ESM2 backbone.

	Learning rate	Batch size	Grad. acc. steps	TTT steps	LoRA rank r	LoRa α
Fitness prediction						
ESM2 (35M) + TTT	4e-5, **4e-4**, 4e-3	**4**	4, 8, **16**, 32, 64	**30**	-	-
ESM2 (650M) + TTT	**4e-5**, 4e-4, 4e-3	**4**	4, 8, **16**, 32	**30**	-	-
SaProt (35M) + TTT	4e-5, **4e-4**, 4e-3	**4**	4, **8**, 16, 32	**30**	-	-
SaProt (650M) + TTT	**4e-5**, 4e-4, 4e-3	**2**, 4	4, 8, **16**, 32	**30**	-	-
Structure prediction						
ESMFold + TTT	**4e-4**	**4**	**4**, 8, 32, 64	**30 (max pLDDT)**	4, **8**, 32	8, 16, **32**
ESM3 + TTT	1e-4, 4e-4, **1e-3**	**2**	**1**, 4, 16	**50 (max pLDDT)**	-	-
Function prediction						
TerpeneMiner + TTT	**4e-4**, 1e-3	**2**	**2**, 4, 8	**30**	-	-
Light attention + TTT	4e-4, 1e-3, **3e-3**	**2**	**2**, 4	**30**	-	-

Light attention + TTT. When applying TTT to Light attention, we treat the frozen ESM-1b as the backbone f, the language modeling head of ESM-1b as the self-supervised head g, and the Light attention block as the fine-tuning head h.

B EXTENDED RESULTS

In this section, we provide additional results on test sets (Appendix B.1) and discuss validation performance (Appendix B.2).

B.1 DETAILED TEST PERFORMANCE

In this section, we provide details on the test performance. Specifically, Table 5 shows that test-time training (TTT) primarily enhances performance on challenging targets, characterized by a low number of similar proteins in sequence databases, as measured by MSA depth. Additionally, we provide an example illustrating how TTT substantially improves the correlation between ESM2-predicted fitness and ground-truth stability by better identifying disruptive mutations within the protein core (Figure 8).

Next, Figure 9 shows the distribution of TTT effects: in many cases, TTT has minimal impact on performance; often, it leads to substantial improvements; and in rare cases TTT results in a decrease in performance. This positions TTT as a method for enhancing prediction accuracy, while a comprehensive analysis of its failure modes remains an important direction for future research. While we demonstrate these effects using a protein folding example, we observe a similar distribution of TTT impact across the tasks.

We also observe that the overall trend of TTT generally leads to improved performance, with robust consistency across random seeds. However, the progression of the performance curve can be rugged, particularly in classification tasks, where substantial changes in the underlying representations are required to shift the top-predicted class in the discrete probability distribution (Figure 10).

B.2 VALIDATION PERFORMANCE

This section discusses the performance of test-time training (TTT) on validation data. Table 6 illustrates the validation performance of all tested methods for fitness prediction on our newly constructed MaveDB dataset. TTT enhances the performance of all the methods.

The primary focus of the section is hyperparameter tuning. Table 4 provides the grid of hyperparameters explored for each model and its size. Figure 11 demonstrates the trend of hyperparameter tuning with optimal hyperparameter combination balancing underfitting and overfitting to a single test protein. While most hyperparameter configurations lead to overall improvements when using TTT, poorly chosen hyperparameters can have detrimental effects due to rapid overfitting. However, with a reliable predicted confidence measure, such as pLDDT, the appropriate TTT step can be selected to mitigate overfitting. Figure 12 demonstrates that when using ESM3 + TTT with pLDDT-based step selection for protein folding, all hyperparameter configurations result in improved performance compared to the base ESM3 model.
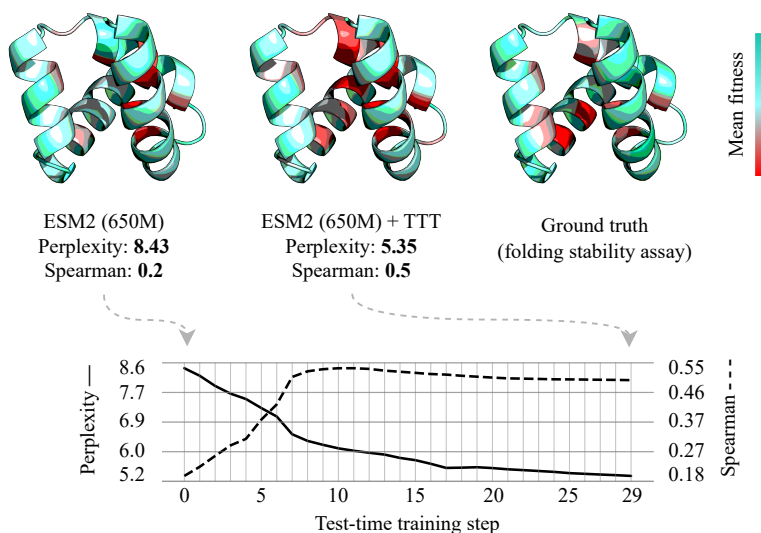

Figure 8: **Example of test-time training (TTT) applied to fitness prediction.** Fitness predictions from ESM2 (650M) show poor correlation with experimental fitness values in the ProteinGym test set measured by the stability assay "UBR5_HUMAN_Tsuboyama_2023_1I2T" (Tsuboyama et al., 2023) (left). ESM2 + TTT achieves significantly higher correlation, likely due to improved detection of disruptive mutations in the protein core that impact protein stability (middle). The ground-truth fitness data aligns with the TTT-enhanced model, showing that residues crucial for stability (i.e., having negative mean fitness) are concentrated in the protein core (right). Residue colors represent the mean fitness upon all single-point substitutions (with the exception of several missing mutations in the ground-truth data), with red indicating residues where mutations have detrimental effects on average.

Table 5: **Test-time training (TTT) performance on ProteinGym depending on MSA depth.** MSA depth reflects the number of available proteins similar to the target protein and, when using large protein language models, can be interpreted as a measure of the representation of similar proteins in the training data (Appendix A.1.2). TTT primarily improves performance on difficult targets, with low MSA depth. Standard deviations are calculated over 5 random seeds but are omitted in the right panel for brevity, where the maximum standard deviation does not exceed 0.0004.

	Avg. Spearman ↑	Spearman by MSA depth ↑		
		Low depth	Medium depth	High depth
ESM2 (35M) (Lin et al., 2023)	0.3211	0.2394	0.2707	0.451
ESM2 (35M) + TTT (Ours)	**0.3407 ± 0.00014**	**0.2445**	**0.3144**	**0.4598**
SaProt (35M) (Su et al., 2023)	0.4062	0.3234	0.3921	0.5057
SaProt (35M) + TTT (Ours)	**0.4106 ± 0.00004**	**0.3253**	**0.3972**	**0.5091**
ESM2 (650M) (Lin et al., 2023)	0.4139	0.3346	0.4063	**0.5153**
ESM2 (650M) + TTT (Ours)	**0.4153 ± 0.00003**	**0.3363**	**0.4126**	0.5075
SaProt (650M) (Su et al., 2023)	0.4569	0.3947	**0.4502**	**0.5448**
SaProt (650M) + TTT (Ours)	**0.4583 ± 0.00001**	**0.3954**	0.4501	0.5439

Table 6: **Performance of test-time training (TTT) on the MaveDB dataset.** In this work, we use our newly constructed MaveDB benchmark as a validation fold for tuning the hyper-parameters of TTT for fitness prediction. For computational efficiency, we only select a subset of 50 proteins (Appendix A.1.1) and do not run TTT across multiple random seeds to estimate standard deviations. The performance shown was calculated by first aggregating correlations per assay, and then per protein (some assays correspond to the same protein).

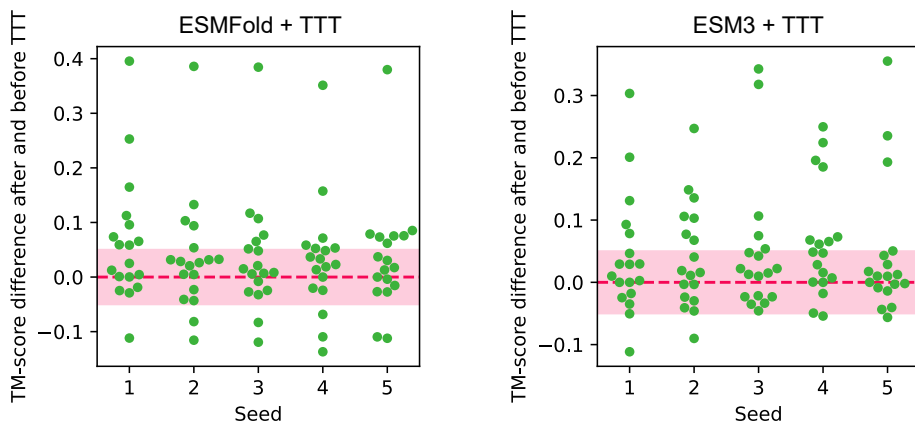|	Avg. Spearman ↑
ESM2 (35M) (Lin et al., 2023)	0.4458
ESM2 (35M) + TTT (Ours)	**0.4593**
ESM2 (650M) (Lin et al., 2023)	0.4568
ESM2 (650M) + TTT (Ours)	**0.4604**
SaProt (650M) (Su et al., 2023)	**0.4926**
SaProt (650M) + TTT (Ours)	**0.4926**
SaProt (35M) (Su et al., 2023)	0.5251
SaProt (35M) + TTT (Ours)	**0.5271**

Figure 9: **Per-protein performance of ESMFold + TTT and ESM3 + TTT on the CAMEO test set.** The y-axis shows the change in TM-score after applying test-time training (TTT), with higher values indicating improvement. The x-axis represents performance across five random seeds. The red dashed line marks no change in TM-score (TM-score difference = 0), and the pink band represents minor changes in TM-score ($-0.05 <$ TM-score difference < 0.05), which we do not consider significant. Each point in the swarm plot corresponds to a single protein from the CAMEO test set. On average, applying TTT to ESMFold improves the structure predictions for 7 out of 18 proteins, with 2 showing degradation. The rest of the proteins are not significantly affected. Similarly, applying TTT to ESM3 results in 6 improvements out of 18 proteins, with 1 case of degradation.
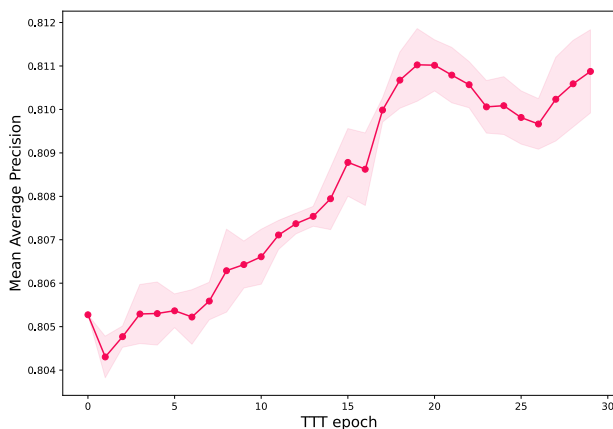

Figure 10: **Test performance of TerpeneMiner + TTT across fine-tuning steps.** The performance is averaged across all 512 proteins in the dataset, with error bars representing the standard deviation across 5 random seeds.
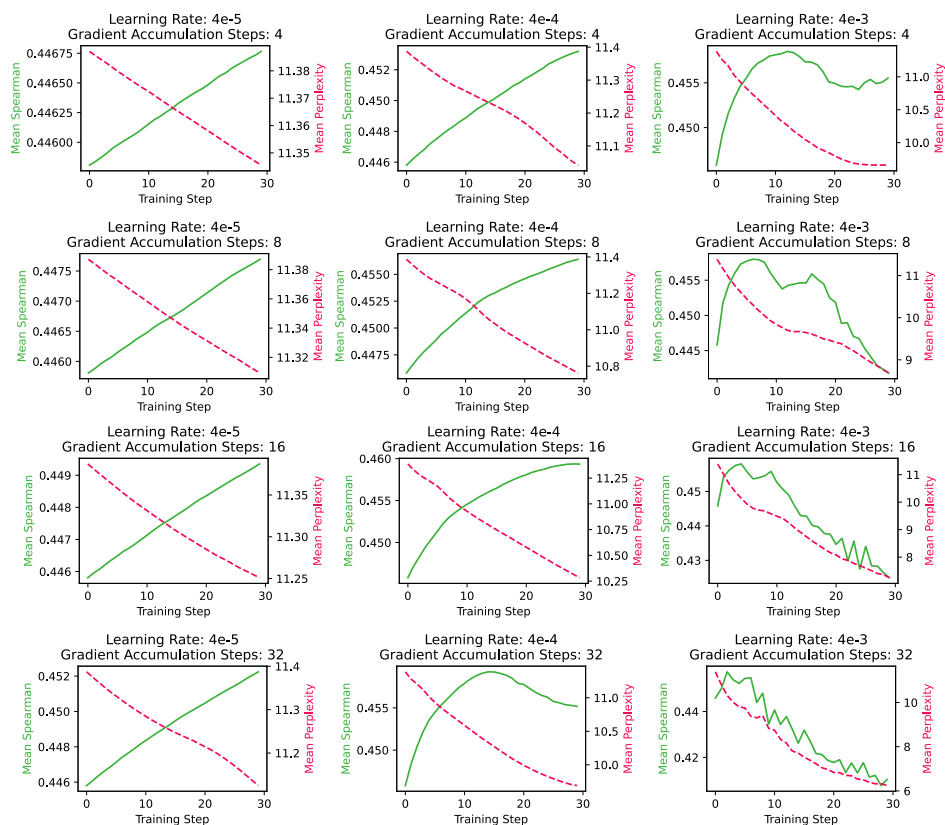
Figure 11: **Dependence on hyperparameters in test-time training for fitness prediction.** Each plot shows the progression of Spearman correlation (green) increasing alongside a decrease in perplexity (pink) for each TTT step, averaged across all assays in the MaveDB validation dataset. The model used is ESM2 (35M) + TTT and the grid displays the progression for all hyperparameter combinations. As the learning rate increases (left to right) and the effective batch size grows, given by the increased number of gradient accumulation steps (top to bottom), the model reaches peak performance more quickly and begins overfitting to a test protein. The optimal hyperparameter combination (learning rate = 4e-4, gradient accumulation steps = 16) lies near the center of the grid, balancing between underfitting and overfitting to a test protein.
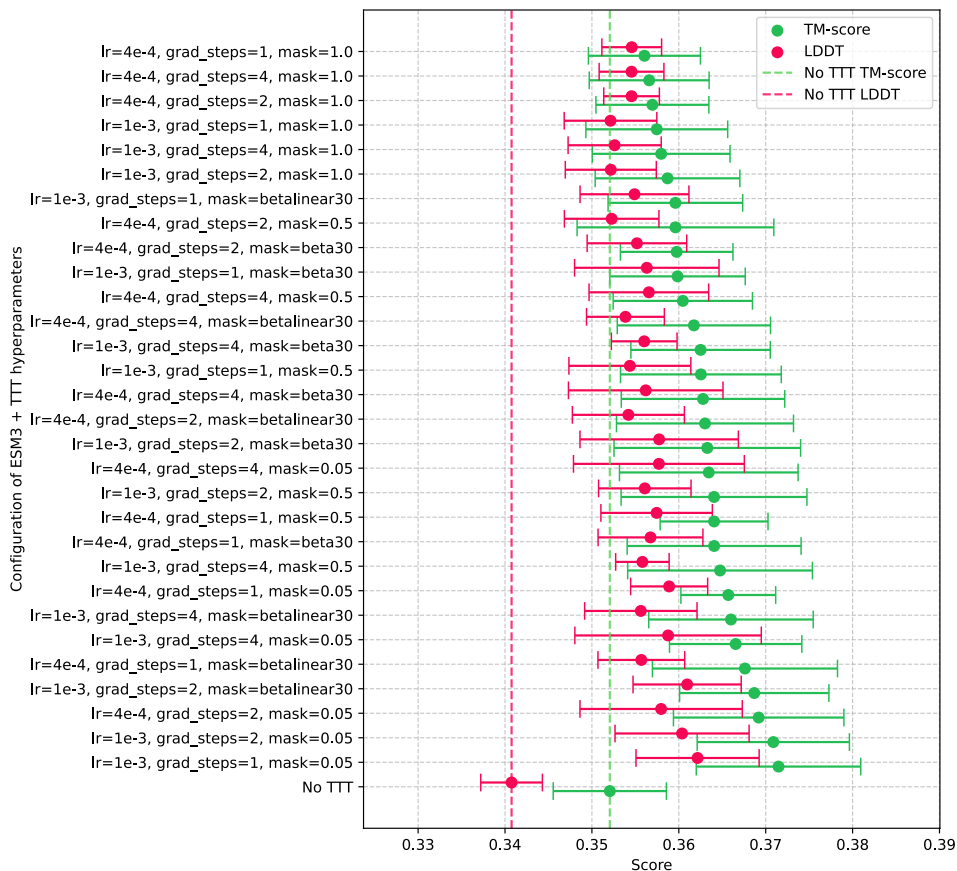
Figure 12: **Hyperparameter search for protein structure prediction with ESM3 + TTT.** We conducted a comprehensive grid search based on three key hyperparameters: learning rate (denoted as "lr"), number of gradient accumulation steps (denoted as "grad_steps"; with the batch size of two), and masking strategy (denoted as "mask"). We explored two learning rates, 4e-4 and 1e-3, three gradient accumulation step values of 1, 4, and 16, and five different masking strategies: uniform sampling of 0.05, 0.5, and 1.0 fractions of amino acids, as well as the beta30 and betalinear30 distributions proposed in the ESM3 paper (Hayes et al., 2024). Each row in the table presents the mean TM-score and LDDT metrics with standard deviations across five random seeds on the CAMEO validation fold. The last row, denoted as "No TTT", shows the performance of ESM3 without TTT. The results indicate that ESM3 + TTT is robust to the choice of hyperparameters and consistently outperforms the base model across all configurations. We selected the configuration from the last row to compute the results on the test fold. For the hyperparameter search, we used 30 TTT steps instead of 50 to reduce computation time.